

University of Montana

ScholarWorks at University of Montana

Graduate Student Theses, Dissertations, &
Professional Papers

Graduate School

1994

Apparent dispersion of a contaminant plume under transient groundwater flow conditions

Viraf Eruch Engineer
The University of Montana

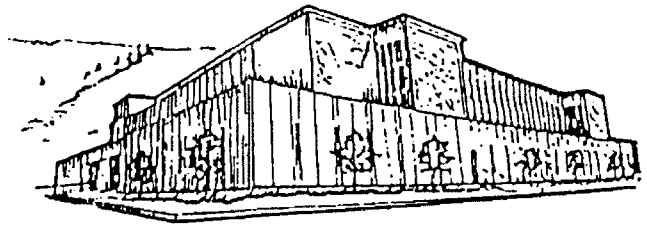
Follow this and additional works at: <https://scholarworks.umt.edu/etd>

Let us know how access to this document benefits you.

Recommended Citation

Engineer, Viraf Eruch, "Apparent dispersion of a contaminant plume under transient groundwater flow conditions" (1994). *Graduate Student Theses, Dissertations, & Professional Papers*. 8993.
<https://scholarworks.umt.edu/etd/8993>

This Thesis is brought to you for free and open access by the Graduate School at ScholarWorks at University of Montana. It has been accepted for inclusion in Graduate Student Theses, Dissertations, & Professional Papers by an authorized administrator of ScholarWorks at University of Montana. For more information, please contact scholarworks@mso.umt.edu.



Maureen and Mike MANSFIELD LIBRARY

The University of
Montana

Permission is granted by the author to reproduce this material in its entirety, provided that this material is used for scholarly purposes and is properly cited in published works and reports.

*** Please check "Yes" or "No" and provide signature***

Yes, I grant permission
No, I do not grant permission

Author's Signature V.E. Engsness
Date: 8/11/94

or commercial purposes or financial gain may be undertaken
author's explicit consent.

APPARENT DISPERSION OF A CONTAMINANT PLUME UNDER
TRANSIENT GROUNDWATER FLOW CONDITIONS

by

Viraf Eruch Engineer

B.S., St. Xavier's College, Bombay, India.

Presented in partial fulfillment of the requirements
for the degree of Master of Science.

University of Montana

June, 1994

Approved by:


Chairman, Board of Examiners


Dean, Graduate School

August 15, 1994
Date

UMI Number: EP39794

All rights reserved

INFORMATION TO ALL USERS

The quality of this reproduction is dependent upon the quality of the copy submitted.

In the unlikely event that the author did not send a complete manuscript and there are missing pages, these will be noted. Also, if material had to be removed, a note will indicate the deletion.

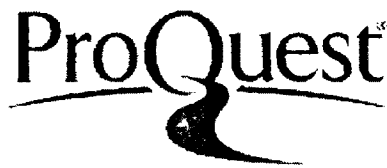


UMI EP39794

Published by ProQuest LLC (2013). Copyright in the Dissertation held by the Author.

Microform Edition © ProQuest LLC.

All rights reserved. This work is protected against unauthorized copying under Title 17, United States Code



ProQuest LLC.
789 East Eisenhower Parkway
P.O. Box 1346
Ann Arbor, MI 48106 - 1346

Apparent Dispersion of a Contaminant Plume Under Transient
Groundwater Flow Conditions *WWW 8-11-94*
(79 pp.)

Director: Dr. William Woessner

This study attempts to quantify and understand the effects of velocity and flowpath variations on the apparent longitudinal dispersion of a contaminant plume. This is done by varying the groundwater flow direction and magnitude of the groundwater velocity, during the transport of a slug injected plume. Apparent dispersion is defined as the spreading of a contaminant plume caused by flow field transients, changes in the flow direction and velocity.

A numerical groundwater flow model of a high hydraulic conductivity aquifer was developed using MODFLOW. The solute transport code MT3D was then used to model plume transport.

Values of longitudinal and transverse dispersivity were fixed at 10 ft. and 1 ft. respectively. Model generated breakthrough curves of the plumes were examined using analytical curve matching techniques developed by Sauty (1980). The resulting longitudinal dispersivity values were then compared to the numerically modeled value of 10 ft. to determine if apparent longitudinal dispersion had occurred.

The model first simulated solute travelling in a straight line under a constant (magnitude and direction) velocity. Another run allowed for a variable magnitude of velocity but maintained a constant flow direction. This was done in order to quantify and understand the effect of the variation in the magnitude of velocity on the longitudinal dispersion of the plume.

The model was then constructed with the magnitude of velocity held constant and the direction of the groundwater flow allowed to vary from 0 to 90 degrees. This was used to quantify and understand the effect of flowpath variation on the longitudinal dispersion of the plume.

Overall the results of this study indicate that variations in groundwater flow direction and magnitude of groundwater velocity within an unconfined aquifer system, cause a increase in the longitudinal dispersivity of a slug injected contaminant plume. These flow field changes allow for a large portion of the the solute to move transversly to the flow direction, thus causing more plume dispersion.

ACKNOWLEDGEMENTS

I would like to thank the geology department for their kind services and encouragement throughout my graduate school years.

My thanks also to the foreign student services on campus for the help and support they provide.

My special thanks goes to Dr. William Woessner. He has been a special teacher and a positive influence on me through these years.

I would also like to thank Dr. Nancy Hinman and Dr. Eijiro Uchimoto for their willingness to take of their time and being on the committee. Their helpful comments allowed me to look at the problem at hand in a better light.

I wish to thank my family and friends everywhere and my partner Kate for their love and support through these years.

Finally, most of all I would like to take this opportunity to recognise the invaluable influence of my parents Eruch and Aban Engineer who have made it possible in their way, for me to come this far. Thanks.

TABLE OF CONTENTS

ABSTRACT	ii
ACKNOWLEDGEMENTS	iii
LIST OF FIGURES	v
LIST OF TABLES	vii
LIST OF APPENDICES	viii
LIST OF PLATES	ix
1.0 INTRODUCTION	1
1.1 PROJECT GOALS AND OBJECTIVES	4
1.2 FIELD SITE BACKGROUND	5
2.0 PREVIOUS RESEARCH	12
3.0 METHODS	21
3.1 MODEL # 1 (FLOW AND SOLUTE TRANSPORT)	23
3.2 MODEL # 2 (FLOW AND SOLUTE TRANSPORT)	25
3.3 MODEL # 3 (FLOW AND SOLUTE TRANSPORT)	28
4.0 RESULTS AND DISCUSSION	39
4.1 MODEL # 1 (FLOW AND SOLUTE TRANSPORT)	39
4.2 MODEL # 2 (FLOW AND SOLUTE TRANSPORT)	39
4.3 MODEL # 3 (FLOW AND SOLUTE TRANSPORT)	42
5.0 CONCLUSIONS AND RECOMMENDATIONS	65
REFERENCES	67
APPENDIX A - Parameters, input files to Model # 1 ..	71
APPENDIX B - Parameters, input files to model # 2 ..	74
APPENDIX C - Parameters, input files to model # 3 ..	77

LIST OF FIGURES

Figure 1	Site Map.....	8
Figure 2	General cross-section of site.....	9
Figure 3 & 4	Potentiometric map of Pottinger's site in June and January.....	10 & 11
Figure 5	Pottinger's variable grid (27 by 26).....	30
Figure 6	Pottinger's site with uniform grid (47 by 52). Also grid system used in Model # 1.....	31
Figure 7	Pottinger's Boundary conditions used in Model # 1.....	32
Figure 8	Potentiometric Map (Model # 1), showing the input point.....	33
Figure 9	Potentiometric Map (Model # 1) showing Section ABCD.....	33
Figure 10	Section ABCD showing grid system used in Model # 2.....	34
Figures 11 to 13	Potentiometric Maps (Model # 2). First, second and third scenarios....	34 & 35
Figures 14 to 17	Potentiometric Maps (Model # 3) for stress periods 1 to 4.....	36 & 37
Figure 18	True and Apparent distances and flowpaths (Model # 3).....	38
Figure 19	Type curves for selected Peclet numbers.....	44
Figures 20 & 21	Plume Maps at 1 and 2 years (Model # 1).....	45
Figures 22 to 26	Breakthrough curves at given locations including at 1 & 2 years (Model # 1).....	46 to 48

Figures 27 to 32	
Plume maps at 1 & 2 years for	
first, second, and third scenarios	
(Model # 2).....	49 to 51
Figures 33 to 38	
Breakthrough curves at 1 & 2 years	
for first, second and third scenarios	
(Model # 2).....	52 to 54
Figures 39 to 46	
Plume maps at selected locations	
(Model # 3).....	56 to 59
Figures 47 to 54	
Breakthrough curves at selected	
locations (Model # 3).....	60 to 64

LIST OF TABLES

Table 1	Summary of longitudinal Dspersivity values. Model # 1.....	48
Table 2	Summary of longitudinal dispersivity values. Model # 2.....	55
Table 3	Summary of longitudinal dispersivity values. Model # 3.....	64

LIST OF APPENDICES

APPENDIX A - Input parameters and files to Flow and Solute Transport Model # 1.....	71
APPENDIX B - Input parameters and files to Flow and Solute Transport Model # 2.....	74
APPENDIX C - Input parameters and files to Flow and Solute Transport Model # 3.....	77

LIST OF PLATES

Plate 1 Input files to Flow and Solute Transport
Models # 1, 2 & 3.

NOTE : All input files stored on computer disk in
pocket at end of report.

1.0 INTRODUCTION

Identifying, characterizing and predicting the fate of groundwater contamination has become the primary focus of private industry and regulatory agencies. Hydrogeologists are often asked to predict the future spatial extent of plumes of contaminants. The accuracy of their predictions depends primarily upon the accuracy of the conceptual model, the groundwater flow within that system, and the chemical changes that will occur during transport.

Many (if not most) analyses of field-scale solute transport problems assume that an average or steady state groundwater flow field prevails (Goode and Konikow, 1990). The usefulness of this assumption has been challenged as plumes in the assumed steady state flow field may also be spread during small variations in the flow field. Thus, estimates of plume spreading mechanisms are incompletely represented and the future predictions of plume behavior are in error.

Naff et al. (1989) postulated that small scale velocity transients may be responsible for large transverse spreading observed at two intensively studied sites. They concluded that changes in the flow field call for adjustments in the transverse dispersion component.

Kinzelbach and Ackerer (1986) illustrated the ability of a steady-flow model to incorporate the dispersive effects of transient flow on solute transport by increasing transverse dispersion (Goode and Konikow, 1990).

Recently Goode and Konikow (1990) examined the effects of transient conditions on the longitudinal and transverse dispersion of a plume at the Idaho National Engineering Laboratory (INEL) modelled earlier by Robertson (1974). They postulated that measurable apparent transverse spreading would be found. However, changes in model design and the actual source history obscured the effect of transient conditions on model results.

Their work concludes that when flow field transients are not recognized or accounted for in solute transport simulations, field-data derived estimates of transverse and longitudinal dispersivity are significantly overestimated. As a result, predictions based on these values are incorrect (Goode and Konikow, 1990).

This study makes an attempt to quantify and understand the effects of velocity and flowpath variations (transient conditions) on the apparent longitudinal dispersion of a contaminant plume. In general, this study attempts to quantify the error involved in predicting the longitudinal dispersive properties of aquifers when transient conditions such as changing velocities and flowpaths in a groundwater flow system are neglected. I use **flowpath** to mean the actual or true path of the plume in the field. The plume disperses along its flowpath.

Generally, a constant velocity and straight line flowpath is assumed when analyzing plume geometry and breakthrough

curves. But in reality, for a plume that actually travels along a path due that has minor and major transient variations in the magnitude and orientation of velocity vectors, additional dispersion occurs. Comparisons of numerically simulated plumes and analytical plume models provide a method to quantify the **"apparent dispersion"**.

I use apparent dispersion as the values of dispersion calculated from analysis of plume geometry, assuming the plume traveled along a linear flowpath from the source to its observed location.

The plumes are modeled as a **slug** of the solute, injected into a high hydraulic conductivity unconfined aquifer.

Mechanical dispersion is assumed to be the principal process operating. The solute is assumed to be a non-reactive or a conservative solute for the purpose of this research.

The model is run first with the solute travelling in a straight line under a constant (magnitude and direction) velocity and then with solute travelling through a field having variable magnitude of velocity but constant direction. **This was done in order to quantify and understand the effect of the variation in the magnitude of velocity on the longitudinal dispersion of the plume.**

The model was then run with the magnitude of velocity held constant and the direction or the flowpath of the groundwater was made to vary from 0 to 90 degrees. **This was done in order to quantify and understand the effect of**

flowpath variation on the longitudinal dispersion of the plume.

The analytically derived results of longitudinal dispersivity were then compared to each other and to the model input value for longitudinal dispersivity which was 10 feet.

My work shows traditional techniques used to analyse plume spreading behavior in a variable velocity field and plumes that have undergone shifts in flowpath directions during transport, yield apparent longitudinal dispersion values that exceed the model input value.

1.1 PROJECT GOAL AND OBJECTIVES

The goal of this project is to quantify the effects, that fluctuations in groundwater velocity and flowpath have on the magnitude of field-based predicted values of apparent longitudinal dispersion.

Specific objectives include the following :

- 1) Development of a simplified one layer, two dimensional, steady state flow model of a highly conductive, unconfined sand and gravel aquifer within which contaminant plume behavior using plume spreading properties (mechanical dispersion) could be evaluated;
- 2) Development of a submodel that reflects the characteristics of a more regional model, and to examine the effects of cell discretization on analysis of plume spreading properties (mechanical dispersion);

- 3) Application of standard analytical tools to assess plume break through curves;
- 4) Determination of the magnitude of apparent and true longitudinal dispersivity values, resulting from variations in magnitude and orientation of velocity and,
- 5) Assess the implications of study results on predicting contaminant behavior in a highly conductive, sand and gravel aquifer.

1.2 FIELD SITE BACKGROUND

I have chosen to test the influence of velocity changes and flowpath variation on plume behavior for the high hydraulic conductivity, unconfined Missoula Aquifer located in western Montana. This aquifer consists of sand, gravel and cobbles deposited by high energy fluvial systems or also referred to as river deposits, along with lake deposits due to the emptying and filling of Glacial Lake Missoula (Alt and Hyndman, 1986).

I have chosen to simulate flow in a sub-region of the aquifer in which large seasonal variations in flow direction occur naturally. I will attempt to evaluate the importance and study the effect of both magnitude and orientation of velocity variations on the dispersion of a theoretical contaminant plume.

This two square mile sub-region of the aquifer is located along the northern edge of the Missoula intermontaine basin,

near the confluence of Grant Creek and the Missoula valley (Figure 1). The alluvial fan deposits associated with Grant Creek are predominantly sand and gravel on the surface and contain some clay lenses at depth. These deposits interfinger with coarse sand, gravel and cobbles from the Clark Fork River system (Figure 2).

Pottinger (1988) showed that groundwater flow directions in the study area fluctuated from approximately due south in June 1985 to west-southwest in January 1986 (Figures 3 & 4). He reported that the recharge from Grant Creek in spring and early summer created a groundwater high in the northern section of the study area and forced the groundwater to flow south. During the fall and winter the rate of recharge from the influent Grant Creek declined, allowing the development of a westward component of flow in the southern section of the study area. This caused the overall direction of groundwater flow to be changed to the west-southwest direction. This flow field has a seasonal flow direction variation of approximately 60 degrees. Goode and Konikow (1990) showed a cyclic variation in a theoretical flow field that varied 20 degrees and caused measurable apparent dispersion to occur.

Clark (1986) determined the following generalized hydrologic properties for the entire Missoula Valley Aquifer: 19.7% for porosity, 11.5% for specific yield, 8.2% for specific retention, and 1,386 ft/d for average hydraulic conductivity.

Armstrong (1991), set porosity values at 20 % for coarse grained layers (Woessner, 1988), and at 35 % for fine grained layers. He states that both these values are representative of porosity for unconsolidated sediments (Davis and DeWiest, 1966; Freeze and Cherry, 1979).

Pottinger (1988) determined the average hydraulic conductivity to be 696 ft/d along with his calibrated values that ranged from 100 ft/d to 1400 ft/d. His average transmissivity value was 767,375 ft/d for the study site.

Miller (1990) states that his values of hydraulic conductivity generally agree with Pottinger's (1988) values, with the exception of the area near the Clark Fork where his values ranged from 3000 to 9000 ft/d.

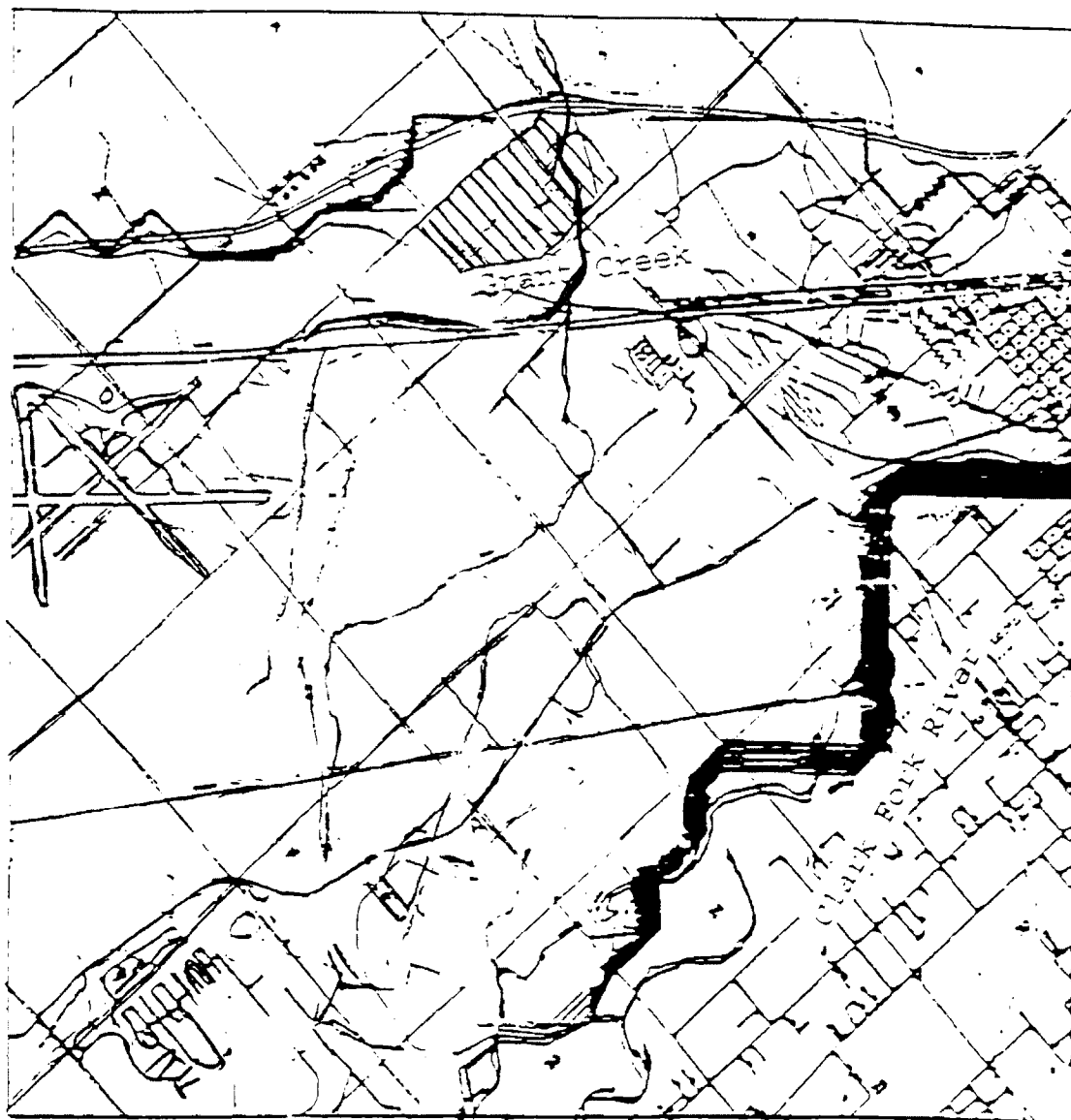


Figure 1. Site map showing the Clark Fork River and Grant Creek.

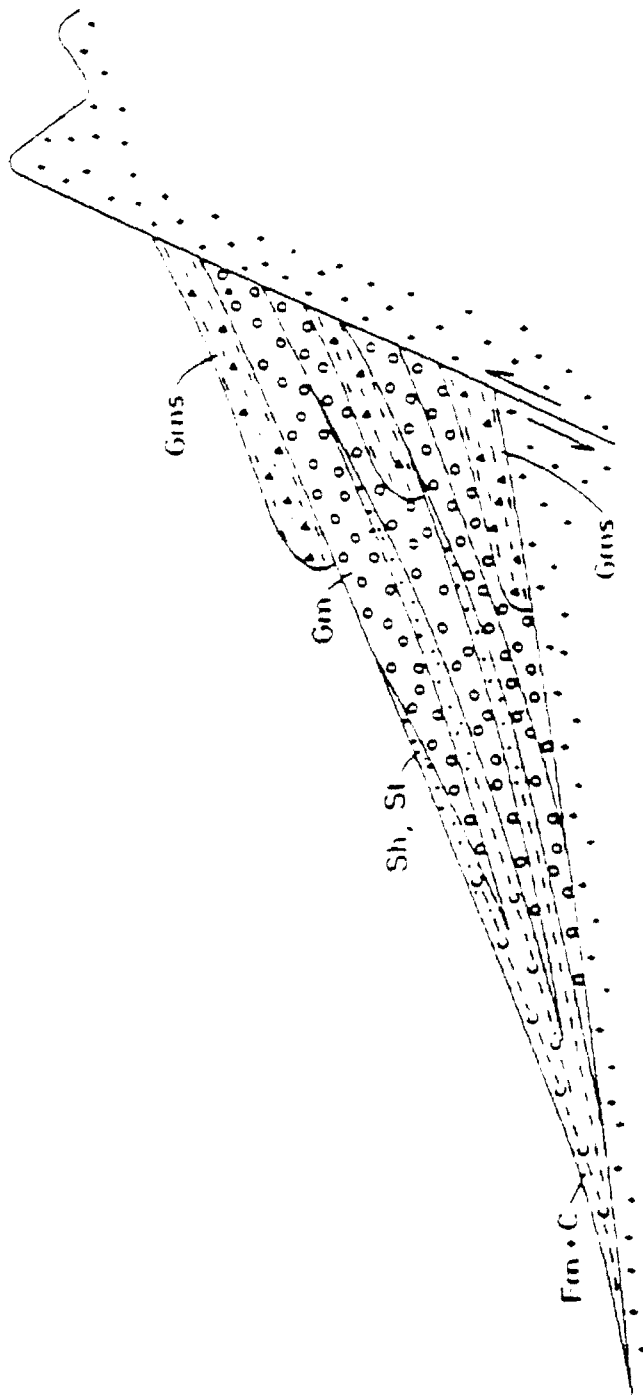


Figure 2. General cross-section of site showing alluvial fan deposits similar to those found in the study area (Walker, 1979).

- Gms - gravels, silt and sand.
- Gm - gravels.
- St - sand
- Sh - silt
- Fm + C - sand and silt
- - Fine grain volcanoclastics.

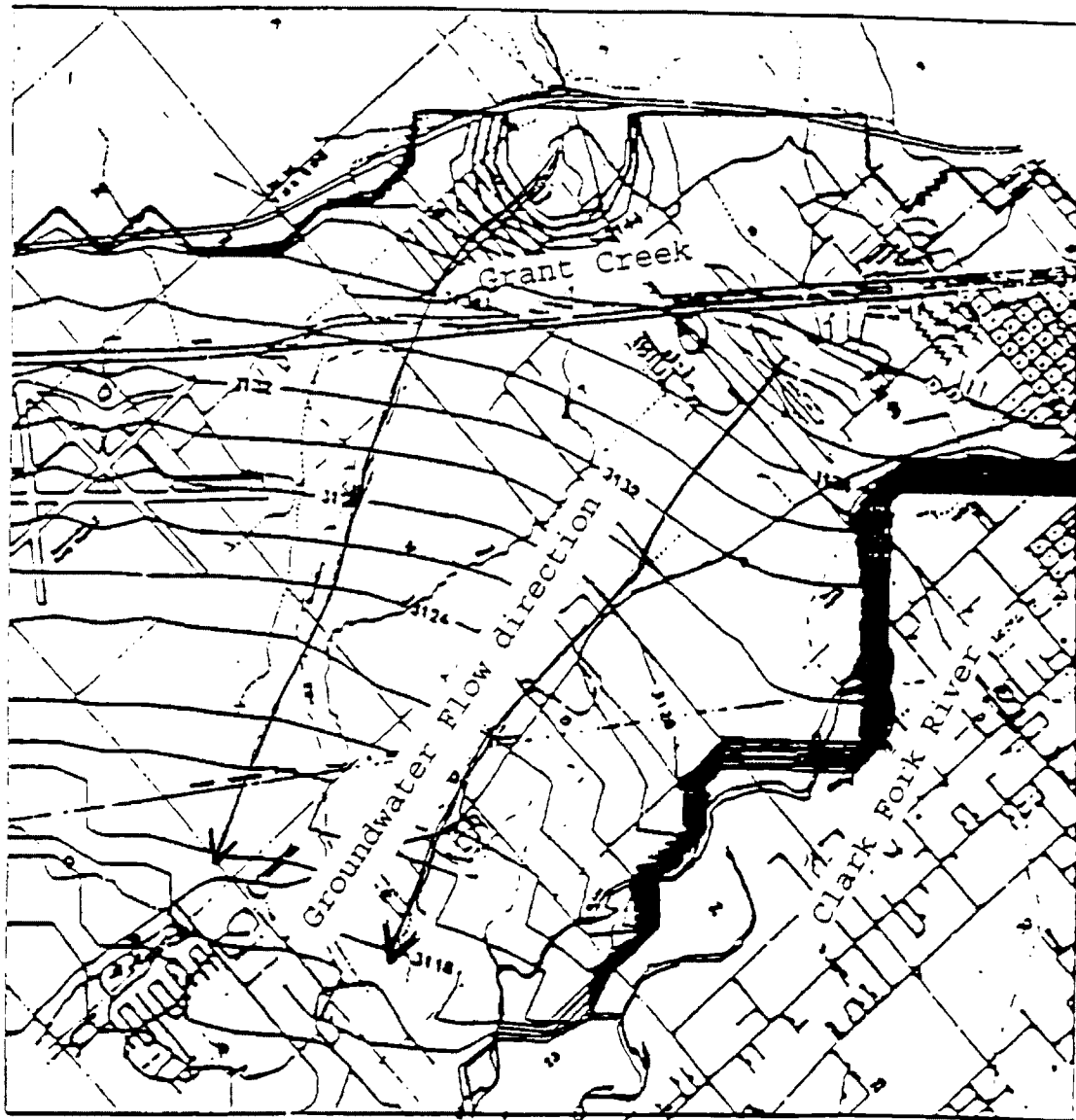


Figure 3. Pottinger's computer generated potentiometric map of site in January showing groundwater flow direction.

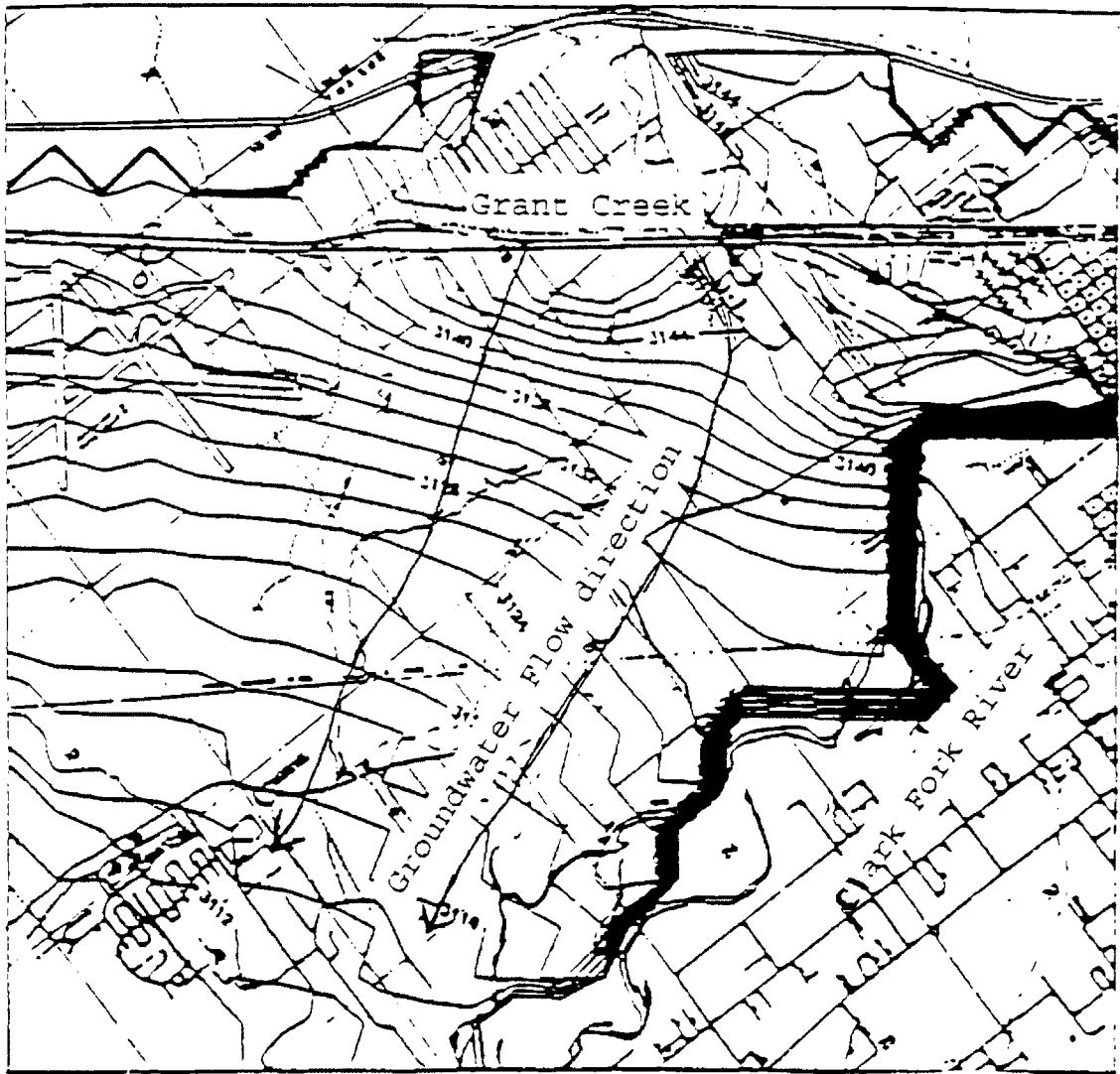


Figure 4. Pottinger's computer generated potentiometric map of site in June showing groundwater flow direction.

2.0 PREVIOUS RESEARCH

Dissolved solids are carried along with flowing groundwater. When the concentration of the solute in the groundwater remains constant in time, and only moves along with the general groundwater flow, then this process is called **advection**. However, when the invading solute-containing water is not all travelling at the same velocity, mixing occurs along the flowpath. Hence a zone of mixing gradually develops around the position of the advective front. This mixing is called **mechanical dispersion** and it results in a greater dilution of the original concentration of the solute in time.

The partial differential governing equation used to describe three-dimensional transport of contaminants in groundwater also known as the advection-dispersion equation can be written as:

$$R \frac{\partial C}{\partial t} = \sum_{i,j} \frac{\partial}{\partial x_i} [D_{ij} \frac{\partial C}{\partial x_j}] - \sum_i \frac{\partial}{\partial x_i} [v_i C] + \frac{q_s}{\theta} C_s - \lambda [C + \frac{\rho_b}{\theta} \bar{C}] \quad (1)$$

where C = Concentration of contaminants dissolved in groundwater, ML^{-3} ;

t = time, (T) ;

x_i = Distance along the respective Cartesian coordinate axis, L ;

D_{ij} = Hydrodynamic Dispersion coefficient, L^2T^{-1} ;

V_i = Seepage or linear pore water velocity, LT^{-1} ;

q_s = Volumetric flux of water per unit volume of

aquifer representing sources (positive) and sinks (negative), T^{-1} ;

C_s = Concentration of sources or sinks, ML^{-3} ;

θ = Porosity of the porous medium, dimensionless ;

ρ_b = Bulk density of the porous medium, ML^{-3} ;

C = Concentration of contaminants sorbed in the porous medium, MM^{-1} ;

λ = Rate constant for the first-order rate reactions, T^{-1} .

R = Retardation factor.

(MT3D document, page 2-2, 1990) .

Equation (1) is the governing equation underlying the numerical and analytical solute transport model, MT3D (Zheng, 1990) .

The transport equation is linked to the flow equation through the relationship (MT3D document, pp. 2-2, 1990) :

$$v_i = -\frac{K_{ii}}{\theta} \frac{\partial h}{\partial x_i} \quad (2)$$

where, K_{11} = Principal component of the hydraulic conductivity tensor, LT^{-1}

h = Hydraulic head, L.

The hydraulic head is obtained from the solution of the three-dimensional groundwater flow equation (MT3D document, pp. 2-3, 1990) :

where, S_s = Specific storage of the porous materials, L^{-1} .

$$\sum_{i,j} \frac{\partial}{\partial x_i} [K_{ij} \frac{\partial h}{\partial x_j}] + q_s = S_s \frac{\partial h}{\partial t} \quad (3)$$

Note that the hydraulic conductivity tensor (K) actually has nine components. However it is generally assumed that the principal components of the hydraulic conductivity tensor (K_{11} , or K_{xx} , K_{yy} , K_{zz}) are aligned with the x, y, and z coordinate axis so that the non-principal components become zero. This assumption is incorporated in most commonly used flow models, including MODFLOW (McDonald and Harbaugh, 1988) which is used in this study.

Hydrodynamic dispersion coefficient or the **coefficient of dispersion** is used to describe the solute spreading processes of mechanical dispersion and molecular diffusion as groundwater moves in the flow system. The coefficient of dispersion can be represented by the equation shown below (Anderson, 1984) :

$$D_{ij}^* = D_{ij} + D_d$$

where D_{ij}^* = Coefficient of hydrodynamic dispersion,

D_{ij} = Coefficient of mechanical dispersion, and

D_d = Coefficient of molecular diffusion.

For the purpose of this research the solute was considered to be a conservative solute (non-reactive) and the effect of molecular diffusion (D_d) on solute spreading was considered negligible. Thus the resulting hydrodynamic dispersion coefficient (D_{ij}^*) is only composed of the mechanical dispersion component, D_{ij} .

The process of mechanical dispersion operates both in the direction of flow (**longitudinal dispersion**) and perpendicular to the flow direction (**transverse dispersion**). These processes are active along a groundwater flowpath regardless of its position in space.

I refer to **apparent dispersion** as the magnitude of spreading (apparent longitudinal dispersion in this study) derived from field plumes in groundwater, when a straight line flowpath and constant velocity are assumed in the field. In reality the plume follows a directionally varying flowpath and the magnitude of its velocity is not constant. Thus, **true dispersion** can be defined as the magnitude of dispersion of a contaminant plume when the actual flowpath (straight line or varying) and the true velocity distribution is properly defined. I use **flowpath** to mean the actual path the plume follows in the field as it moves and disperses along with the bulk direction of groundwater flow. The actual path can be a straight line or curved path depending on the existing flow field.

Describing every point in the varying flowpath of the plume and the exact velocity field is impractical for field scale problems and thus straight line flowpaths and constant velocities are generally assumed. The use of a constant velocity and straight line path versus the varying velocity and flowpath distribution of the groundwater flow system is believed to result in an overestimation of the field scale

dispersion.

A one-dimensional analysis of the governing equation **assuming** that the tracer was conservative (i.e. non-reactive, no molecular diffusion), instantaneous in time with a slug source of injection (as opposed to a continuous source of injection), was performed by Sauty (1980) in which he derived the following equations :

$$C_R(t_R, P) = \frac{K}{(t_R)^{1/2}} \exp\left[-\frac{P}{4} t_R (1-t_R)^2\right] \quad (5)$$

where t_R = Dimensionless time

and

$$K = (t_{Rmax})^{1/2} \exp\left[\frac{P}{4 t_{Rmax}} (1-t_{Rmax})^2\right] \quad (6)$$

where

$$t_{Rmax} = (1+P^{-2})^{1/2} - P^{-1} \quad (7)$$

where t_{Rmax} = time of peak concentration.

and

$$C_R = C/C_{max}$$

where C_{max} = peak concentration.

and

$$P = (x/\alpha) \quad (8)$$

where P = Peclet number

α = aquifer dispersivity

x = distance of plume travel.

Normalised breakthrough curves are prepared using this equation and plume breakthrough curves are analysed to

determine the value of longitudinal dispersivity.

In the paper by Sauty (1980) he states that important differences occur between one and two dimensional flow fields when the Peclet number (P) is less than 10. It also states that the use of the correct solution to match field conditions becomes crucial when the Peclet number is less than 10.

Sauty (1980) states that when sampling is done close to the flow axis it leads to better velocity and thus better dispersivity evaluation. Also the finer the discretisation the better the results (less error involved). But, the degree of discretization used for the model grid has to comply with the smallest practical grid spacing that model restrictions, computer storage and available data will allow (Davis, 1987).

Hence, in this research it was important to discretise the grid finer, and align it in the direction of flow to increase accuracy in determining values of dispersivity and not a two dimensional analysis of the same data.

Sauty (1980), concluded that dispersivity obtained from tracer tests is an increasing function of the distance between injection well and sampling well. He concluded that, this function stabilizes when a certain characteristics value is reached, which is the scale of controlling heterogeneity.

Sudicky (1986) examined the effects that the spatial variabilities of hydraulic conductivity had on a long-term tracer test performed in the Borden aquifer. He related the spatial variability of hydraulic conductivity to the

dispersion of the tracer at the site.

Billings (1992) conducted a tracer test at the Elk Creek aquifer site at the Lubrecht Experimental Forest near Missoula, Montana. He related the spatial variability of hydraulic conductivity to the dispersion of the tracer.

"Values calculated from the data close to the point of injection are lower than values calculated from data recorded at larger distances" (Billings, 1993). This trend is consistent with the observed scaling effect of dispersivity described by Cherry et al. (1975), Bredehoeft (1976), Domenico and Robbins (1984), Davis (1986), Newnman (1990) and others.

The general consensus is that dispersion is Fickian near the source of the contaminant, and therefore for small times or small distances from the source, the standard form of the advection-dispersion equation does not apply (Anderson, 1984).

Large variability in dispersion parameters for what appear to be similar aquifers are common.

The standard representation of the dispersion process has ever been called into question, and stochastic and fractal geometry have been called upon to define the dispersion process (Fetter, 1993).

Recently Goode and Konikow (1990) examined the effects of transient conditions on the longitudinal and transverse dispersion of a plume at the Idaho National Engineering Laboratory (INEL) modelled earlier by Robertson (1974). They postulated that measurable apparent transverse spreading would

be found. However, their work concluded that transient conditions had little effect on model results.

Naff et al. (1989) postulated that small scale velocity transients may be responsible for large transverse spreading observed at two intensively studied sites. They concluded that changes in the flow field call for adjustments in the transverse dispersion component.

Kinzelbach and Ackerer (1986) illustrated the ability of a steady-flow model to incorporate the dispersive effects of transient flow on solute transport by increasing transverse dispersion (Goode and Konikow, 1990).

The paper by Goode and Konikow (1990) states that when flow field transients are not recognized or accounted for in steady state simulations, significant overestimates of transverse and longitudinal dispersivity values during model calibration may result, weakening predictive modelling. They concluded that unrecognized flow field transients that change the direction of flow of a plume cause an apparent increase in transverse dispersivity because longitudinal dispersion is not parallel to the assumed direction of flow. They also concluded that increase in transverse dispersivity under transient flow is primarily a function of the extent of change in flow direction and the ratio of longitudinal to transverse dispersivity.

Rehfeldt (1988) applied the stochastic small-perturbation approach of Gelhar and Axness (1983) to investigate solute

transport impacts of temporal variability in the hydraulic gradient (Goode and Konikow, 1990). Both longitudinal and transverse dispersivity were increased by fluctuations in direction and magnitude of velocity, although the effect on longitudinal dispersivity was generally insignificant.

Though research indicates the need to adjust values of dispersivity as distance of travel increases, they have not determined a unified method to make those adjustments.

Thus most previous research concludes that there is an increase in the apparent longitudinal and/or transverse dispersion of a contaminant plume, when subjected to changing conditions of velocity and flowpath (transient conditions), within the groundwater flow system. They also conclude that dispersion of the tracer at a site is directly related to the spatial variability of hydraulic conductivity.

Other researchers have raised the issue that though the factors described above need to be considered, the magnitude of plume spreading that occurs from fluctuating velocity and flowpath within the field is not well explained.

Thus, estimates of plume spreading mechanisms (dispersivities) are poorly approximated and the future predictions of plume behavior are in error.

In this research, I attempt to quantify the effects of a variable velocity field and complex flowpath history on the apparent longitudinal dispersivity calculations.

3.0 METHODS

The main purpose of this research was to quantify the longitudinal dispersion of a theoretical contaminant plume when the groundwater flow field varies due to fluctuating velocity and flowpath, within a highly transmissive unconfined aquifer system.

A groundwater flow model, a solute transport model, a data visualisation program, a worksheet program, and some analytical solutions were applied, to quantify the degree of apparent dispersion.

MODFLOW, a USGS (United States Geological Survey) three-dimensional, finite-difference groundwater flow model is versatile, portable (runs on a wide range of computers), has excellent documentation, and has shown past success of other workers in applying it to regional aquifer studies (McDonald and Harbaugh, 1988).

I managed to successfully apply this model, to create all the flow model input files. The execution was carried out using the MODFLOW executable file (Modf.exe) that has been incorporated within the three dimensional solute transport model, MT3D (Zheng, 1990) and is designed to be used in conjunction with the flow model.

The solute transport models were constructed and executed using the code, **MT3D** (Zheng, 1990). This code was selected because it is virtually free of numerical dispersion and oscillations, flexible for a variety of field conditions, and

is efficient with respect to computer memory and execution time. The code uses a mixed Eulerian-Lagrangian approach to solve the advection-dispersion equation.

The graphics program SURFER (Golden Software, Inc., 1991) was used to create potentiometric maps and plot plume positions.

The worksheet program Quattro (Borland International, Inc., 1987) was used to create graphs (breakthrough curves) of the simulated concentration versus time data for each plume.

Breakthrough curves of the numerically simulated plumes were graphed and matched with a set of dimensionless type curves as described by Sauty (1980).

A one dimensional analysis was performed on the data in order to estimate the longitudinal dispersivity value.

In the paper by Sauty (1980) he states that important differences occur between one and two dimensional flow fields when the Peclet number (P) is less than 10. It also states that the use of the correct solution to match field conditions becomes crucial when the Peclet number is less than 10.

The unusually high value of longitudinal dispersion in Model # 1 was a problem that was solved by a finer discretization of the model grid and aligning the groundwater flow direction with the grid as seen in Models # 2 & 3, rather than a two dimensional analysis of the same data. The results of this can be seen when values of longitudinal dispersivity in Model # 1 are compared to values in Model 2 & 3.

A two dimensional analysis was not necessary in model # 2 and 3 as values of longitudinal dispersivity are nearly identical to the one dimensional values stated in the paper by Sauty (1980).

Sauty (1980) states that when sampling is done close to the flow axis it leads to better velocity and thus better dispersivity evaluation. Also the finer the discretisation the better the results (less error involved). But, the degree of discretization used for the model grid has to comply with the smallest practical grid spacing that model restrictions, computer storage and available data will allow (Davis, 1987). Thus, in this research it was important to discretise the grid better and align it in the direction of flow to increase accuracy in determining values of dispersivity and not a two dimensional analysis of the same data.

The values of longitudinal dispersivity calculated from curve matching was then compared to the value used as model input and to one another.

Three basic models that comprised of both the flow and solute transport simulations were developed for the analysis and are described under sections 3.1, 3.2 and 3.3.

3.1 MODEL # 1 (FLOW AND SOLUTE TRANSPORT)

Model # 1 was constructed to represent Pottinger's (1988) field site. It was used to identify problems of working at a typical field scale and as a tool to design generic small

scale models.

A one layer, two dimensional, unconfined steady state flow model was developed using Pottinger's (1988) field data and his PLASM (Prickett and Lonquist, 1971) flow modeling results. I converted his 27 rows by 26 columns variable grid into a uniform grid with 47 rows and 52 columns (Figures 5 & 6). Cell dimensions of the new model grid were 500 feet by 500 feet. I also used Pottinger's model boundary conditions (Figure 7). The total area represented by the new model grid remained the same. The Clark Fork River was simulated using the river package, and leakage from Grant Creek was simulated using the well package. The model simulated a one year period. The various parameters and names of input files used in the flow simulation are given in detail in Appendix A. The resulting flow field matched with Pottinger's average head data for the year.

The resulting calibrated steady state flow field was used as input to the solute transport code. A starting concentration of 1000 mg/l was input as a slug at location (25,23) = (Row,Col) of the grid (Figure 8). I assigned a constant longitudinal dispersivity value of 10 feet, and the ratio of transverse dispersivity to longitudinal dispersivity was 0.1. The model simulated a three year period. The other parameters and names of input files used in the solute transport simulation are provided in detail in Appendix A.

The results of the solute transport run were then

processed and two dimensional plume maps and breakthrough curves for selected locations along the groundwater flowpath were developed. Breakthrough curves observed at selected distances along the flowpath were then matched to type curves developed from Sauty (1980).

The modeling effort would determine if model data generated and analyzed at this scale would yield acceptable values of apparent longitudinal dispersivity when compared to the actual value used in the model.

In this model the grid and the groundwater flow direction were not aligned. Hence, measuring distance from input point to the centre of the plume was calculated using the Pythagorean theorem approach.

3.2 MODEL # 2 (FLOW AND SOLUTE TRANSPORT)

A section ABCD (7000 feet by 7000 feet) of the initial flow model (Figure 9) was then selected and further discretized into a 70 rows by 70 columns grid with a uniform grid spacing of 100 feet in both directions, for a more detailed analysis of dispersivities calculated from Model # 1 (Figure 10).

This one layer, two dimensional, unconfined, steady state model was used to obtain a more detailed analysis of the changes in the magnitude of the interpreted longitudinal dispersivity values.

In the paper by Sauty (1980) states that for tracer test

interpretation if the sampling well is not close to the flow axis it may introduce errors and result in an incorrect evaluation of velocity and dispersivity. This model was designed such that the flow direction was aligned with the model grid, thus minimizing the error involved in calculating distances. **This would also allow testing of the effect of velocity variation on the predicted plume dispersion under steady state conditions with greater accuracy.**

The second modeling effort involved assessing the magnitude of longitudinal dispersivity that could be accounted if the actual variable velocity distribution within the field was poorly represented.

The equation $V=Ki/n$, shows the relationship between the velocity (V), hydraulic conductivity (K), the gradient (i), and porosity (n). The velocity of groundwater flow within a system can be changed by changing one or more of the above parameters seen in the equation. **Using this equation, the following three scenarios were developed and run independently in this model.**

The **first scenario** involved evaluating the apparent dispersion along a straight line flowpath in a constant velocity flow field. The one layer, two dimensional, unconfined, steady state system aquifer was treated as isotropic and homogeneous. Hydraulic conductivity (K) was set at 700 ft/d. Porosity was a constant value of 0.2 through the model. The resulting flow field is shown (without the overlain

grid) in Figure 11.

In the **second scenario**, the hydraulic conductivity (K) was 700 ft/d for the first 3000 feet of the model, then uniformly changed to 400 ft/d for the next 2000 feet and finally was set to 700 ft/d for the last 2000 feet of flow. Porosity remained at 0.2 throughout the model. As the flux in and out of the model remained constant the flow model simulated hydraulic gradients for each of the constant hydraulic conductivity zones. This resulted in a constant velocity that was less than that of the first scenario. The resulting flow field (without overlain grid) is shown in Figure 12.

The **third scenario** set hydraulic gradients within the flow field using constant head boundaries. A constant value of hydraulic conductivity (K) of 700 ft/d was assigned for the entire model. Porosity remained at 0.2 through the model. This created a model with a systematically varying velocity. The resulting flow field (without overlain grid) is shown in Figure 13.

The solute transport model # 2 had the same initial input for the various parameters as described under "Flow and Solute Transport model # 1". The input point or the point of injection of the slug was (35,6)=(row,column) as shown in Figure 10.

Appendix B contains the input parameters and names of the flow and solute transport input files used in the three

simulations.

The general overall procedure to obtain the potentiometric maps, maps of the various plumes, and the values of longitudinal dispersivity employed here was the same as described in Model # 1.

3.3 MODEL # 3 (FLOW AND SOLUTE TRANSPORT)

This model was used to evaluate the magnitude of **apparent** and **true** longitudinal dispersion in a directionally varying groundwater flow field (fluctuating flowpath).

This one layer, two dimensional, unconfined, **transient** model had the same dimensions as in Model # 2 (Figure 10). The model was designed with four different stress periods each three months long. The flow model simulated a total period of three years, repeating the same annual stress cycle (each cycle = 1 year, each stress period = 3 months) for all three years. By manipulating the two flux boundaries, I changed the flow direction from 0 to 90 degrees. The resulting flow fields for stress periods 1 to 4 (first year) are shown in Figures 14 to 17. The second and third year simulations repeat the same stresses as in the first year cycle, and thus result in the same flow fields as in the first year, and hence are not shown.

The initial or starting heads used in the transient model run were taken from the first scenario of model # 2 (Figure 11). The model represented isotropic and homogenous

conditions with a average hydraulic conductivity of 700 ft/d. The various parameters and names of flow and solute transport model input files are given in detail in Appendix C.

In this model, the **true distance** (X_t) is the actual distance covered by the plume and is measured along the variable flowpath taken by the plume which is its **true flowpath**. The **apparent distance** (X_a) is the distance measured along a straight line between the source and plume center or the plumes **apparent flowpath** as one would measure in the field without prior or accurate knowledge of the groundwater flow directions (Figure 18).

Thus, I calculated two values of longitudinal dispersivity one along its true flowpath and one along its apparent flowpath. They are referred to as **true longitudinal dispersivity** and **apparent longitudinal dispersivity**.

The general overall procedure to obtain the potentiometric maps, maps of the various plumes, and values for longitudinal dispersivity employed here was the same as in Section 3.1, Model # 1.

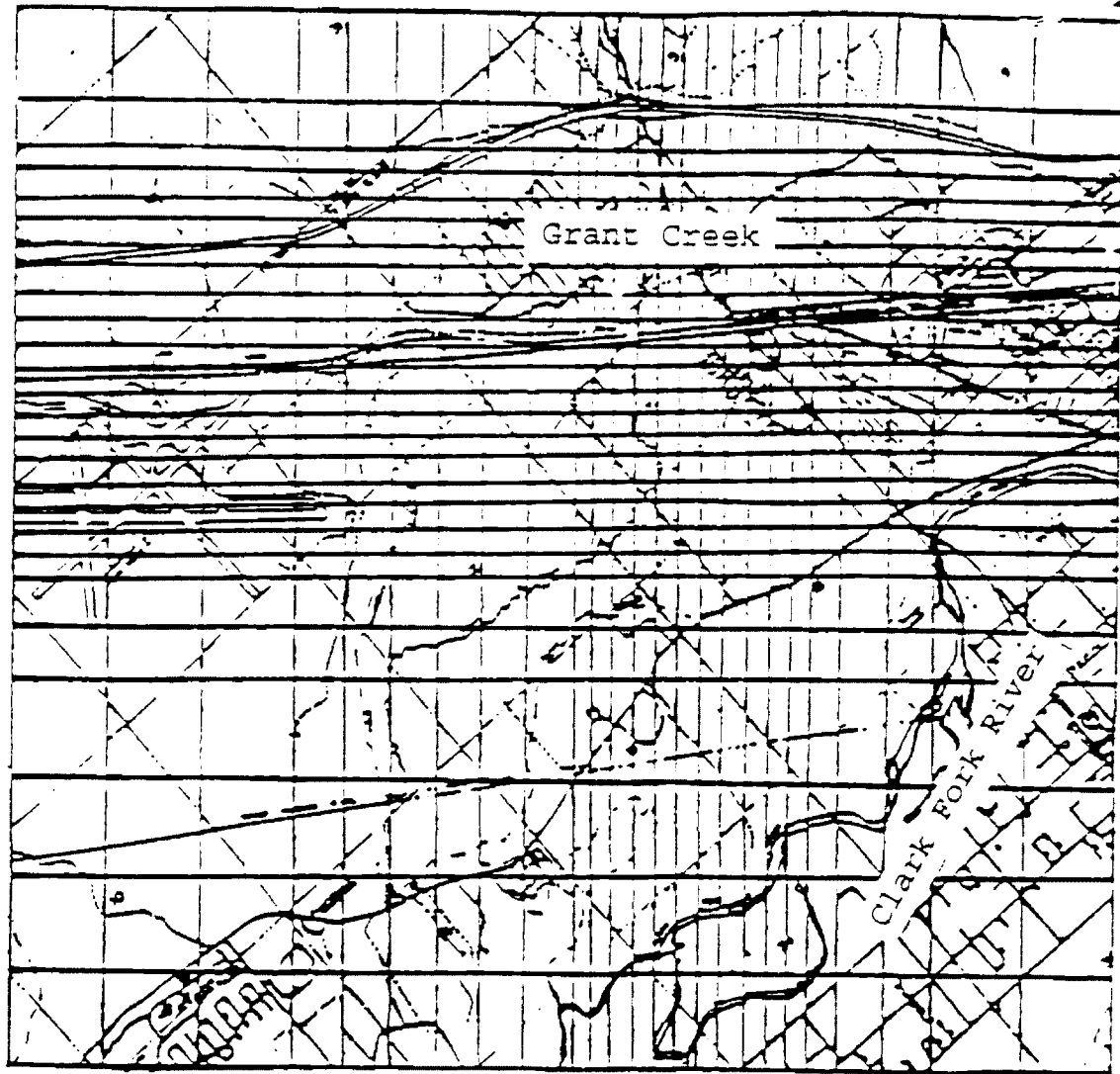
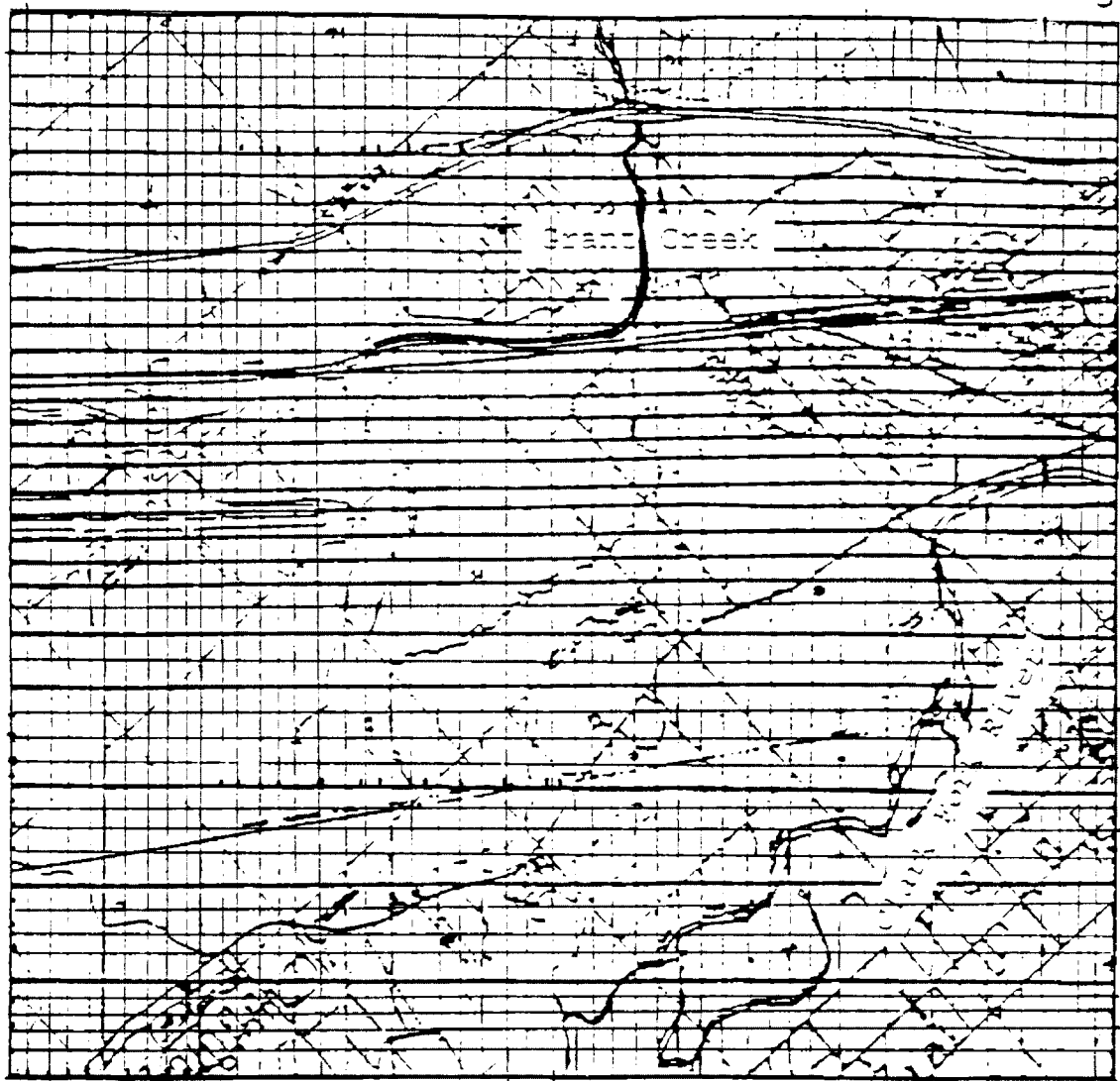


Figure 5. Pottinger's variable grid system over site (27 rows, 26 cols).



51

Figure 6. Uniform grid system used in Model = 1 over the site.



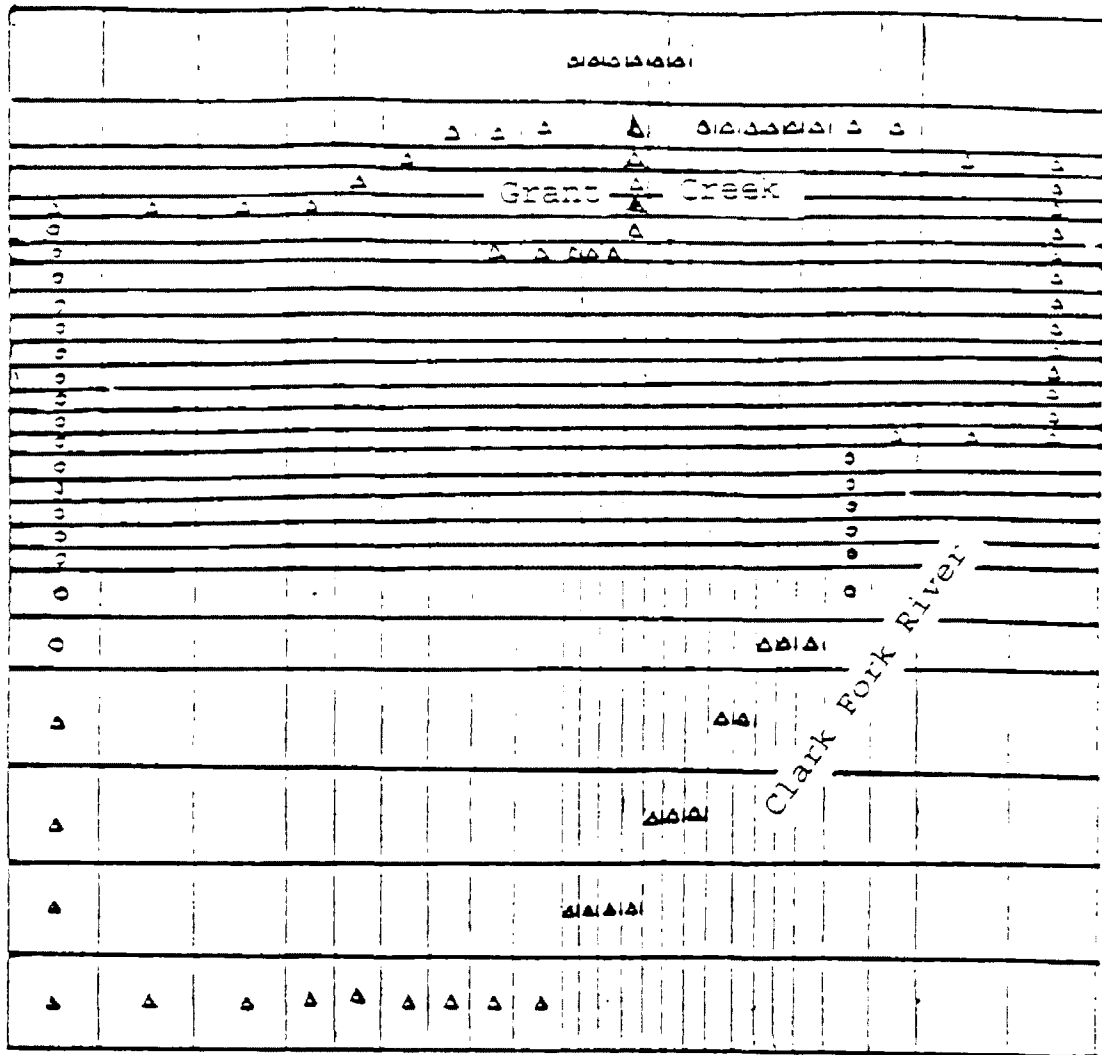


Figure 7. Pottinger's boundary conditions used in Model # 1.

- Δ - constant head
- - no flow

(1,1) = (R₁₀₀, 1) Figure 8. Potentiometric Map (Model # 1)

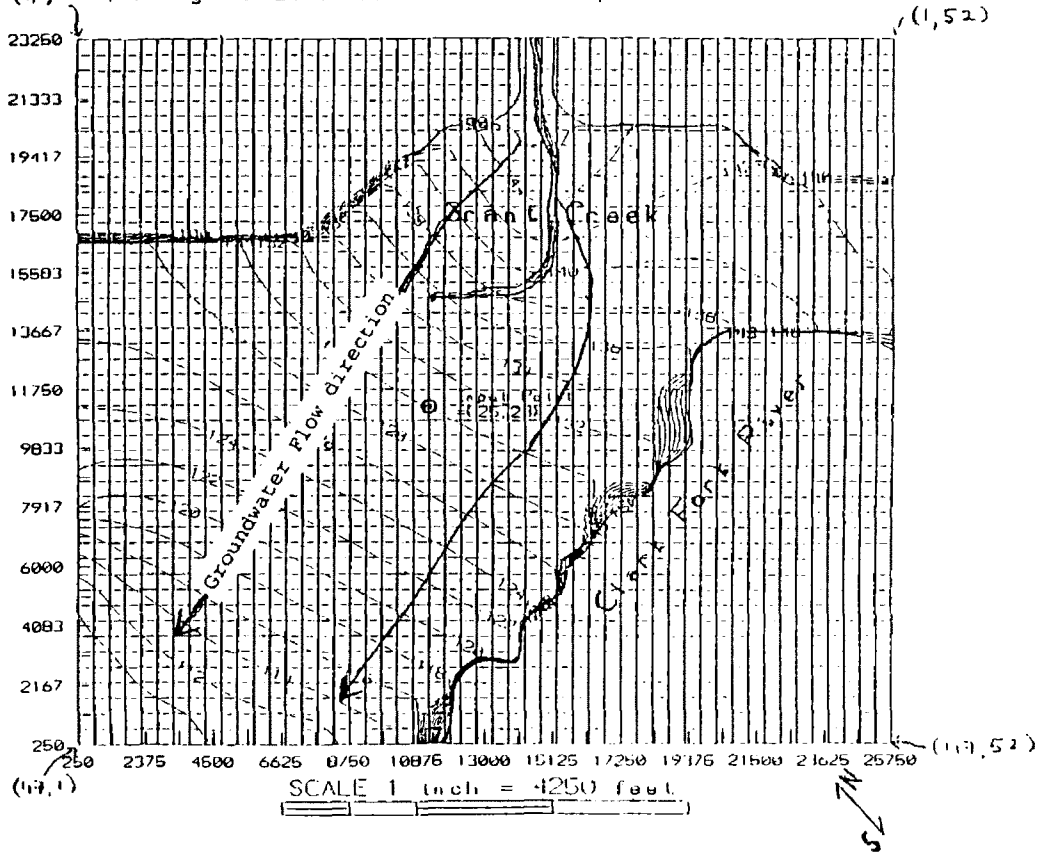


Figure 9. Potentiometric Map (Model #1) showing Section ABCD.

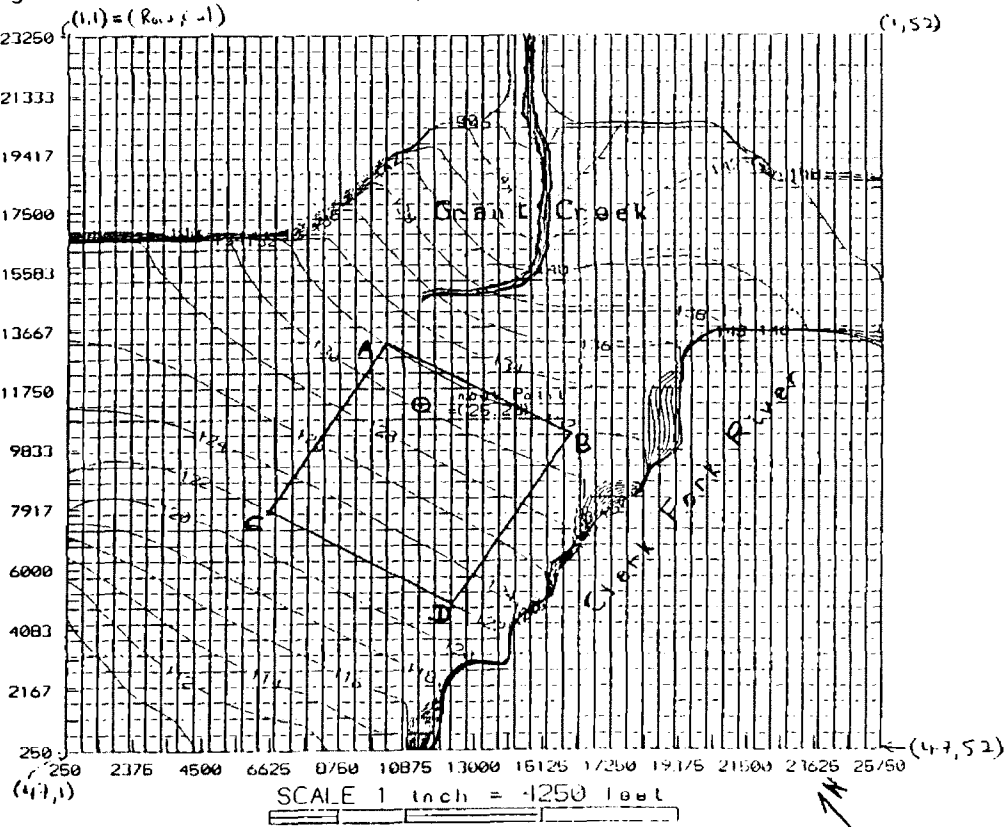


Figure 10. Grid system used in Model # 2 (70 rows, 70 cols)

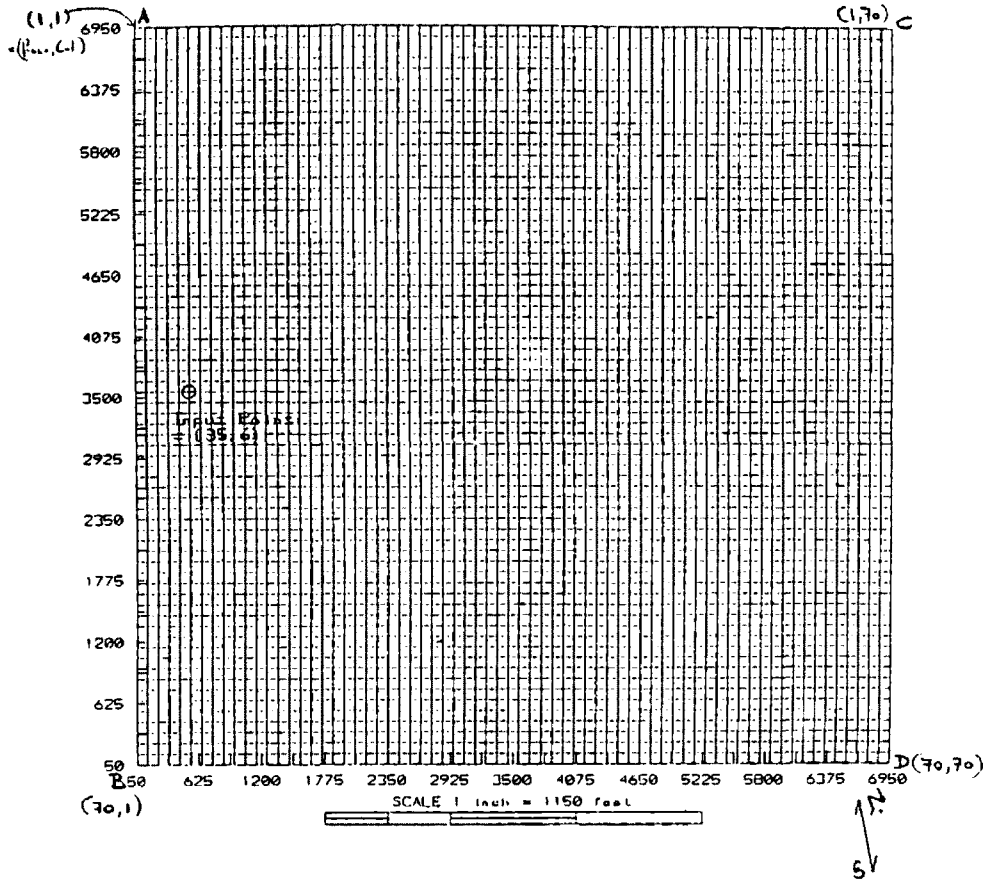


Figure 11. Potentiometric Map (Model # 2, First Scenario)

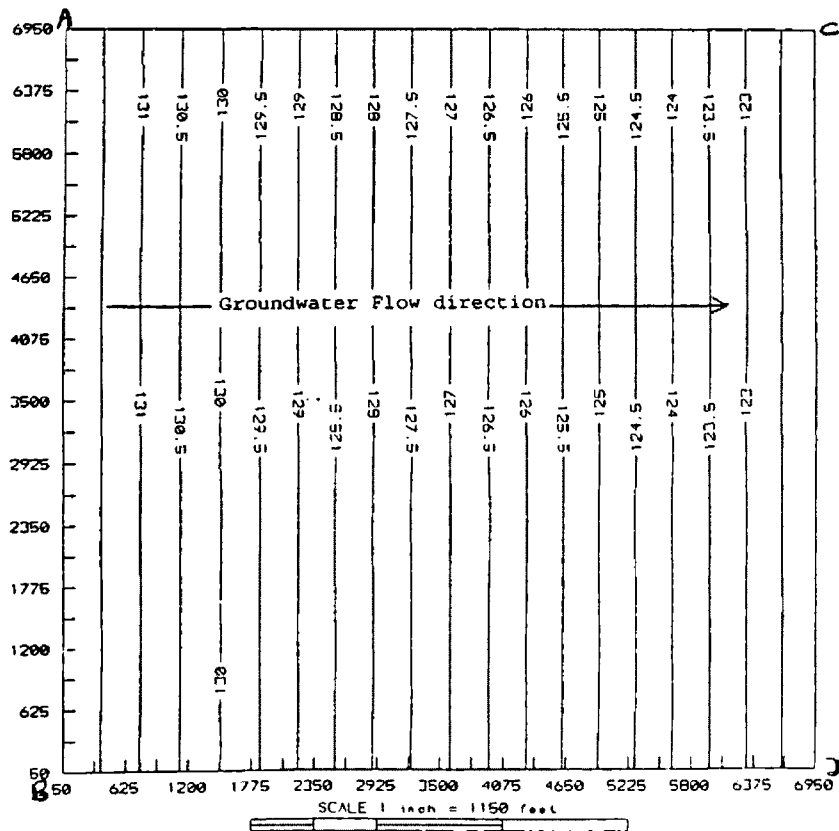


Figure 12. Potentiometric Map (Model # 2, Second Scenario)

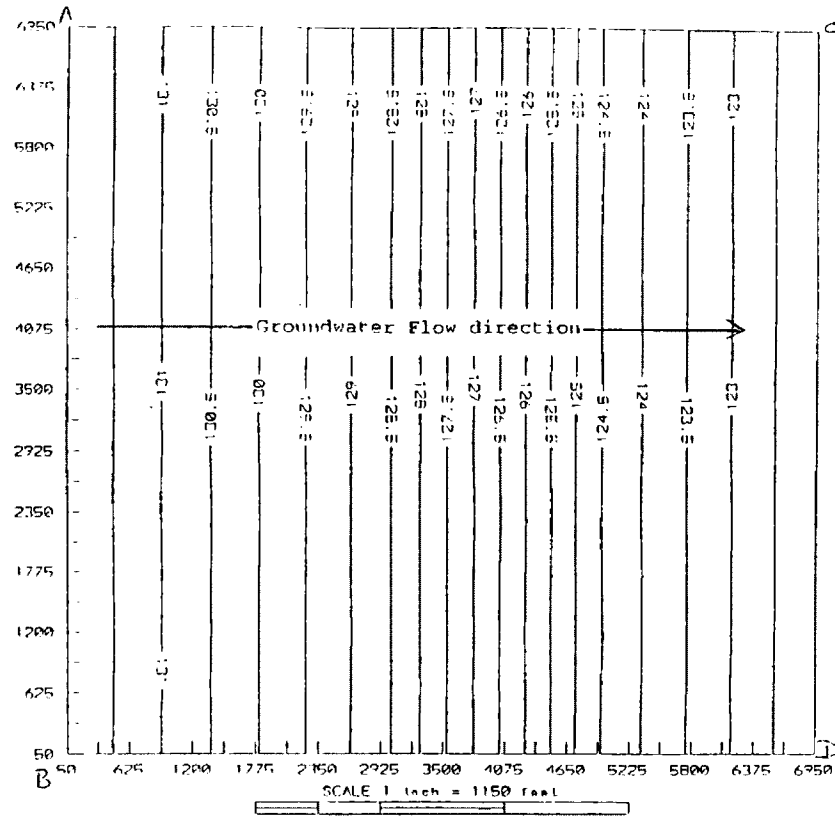


Figure 13. Potentiometric Map (Model # 2, Third Scenario)

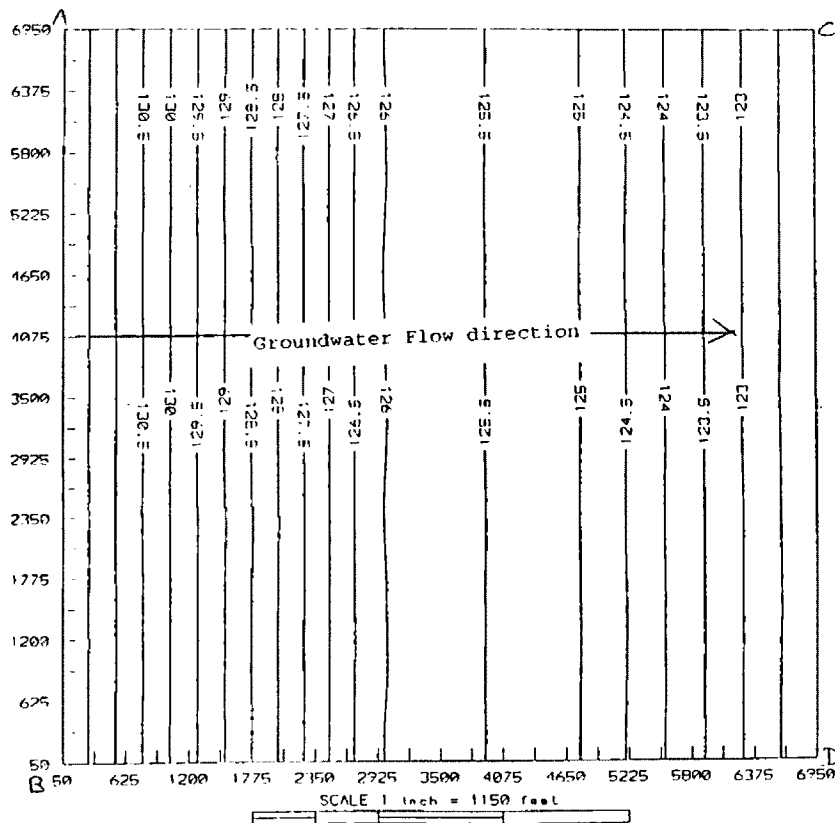


Figure 14. Potentiometric Map (Model # 3, Stress Period 1)

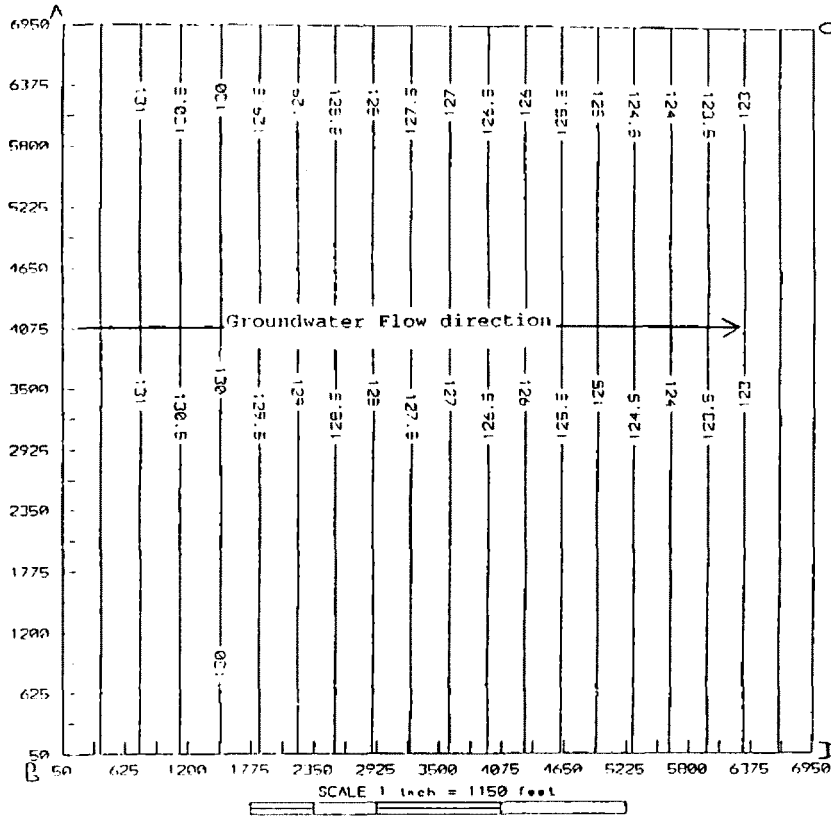


Figure 15. Potentiometric Map (Model # 3, Stress Period 2)

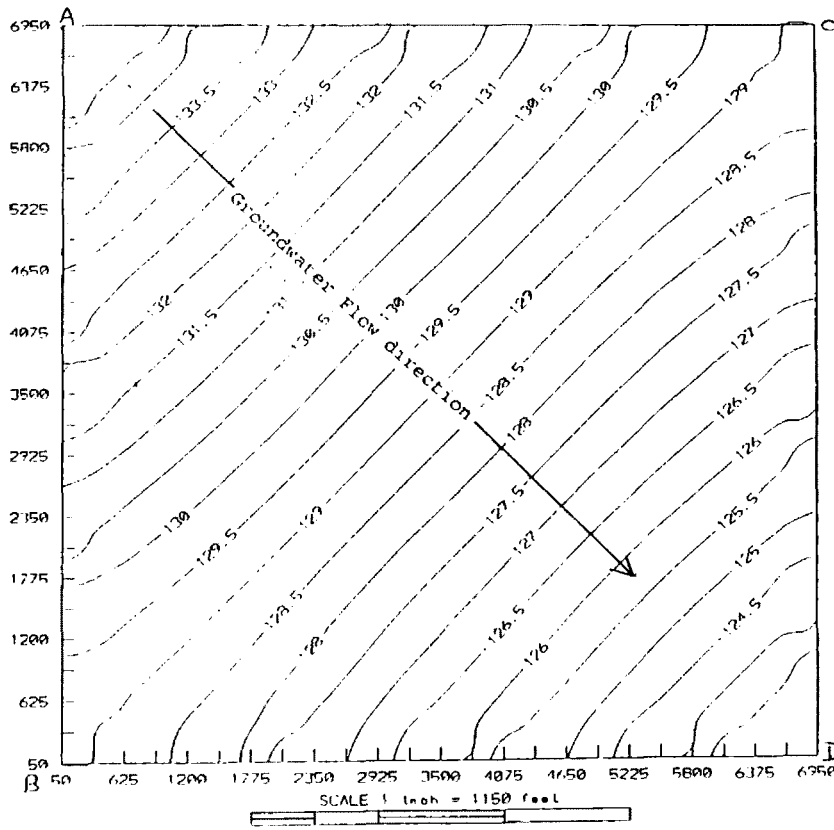


Figure 16. Potentiometric Map (Model # 3, Stress Period 3)

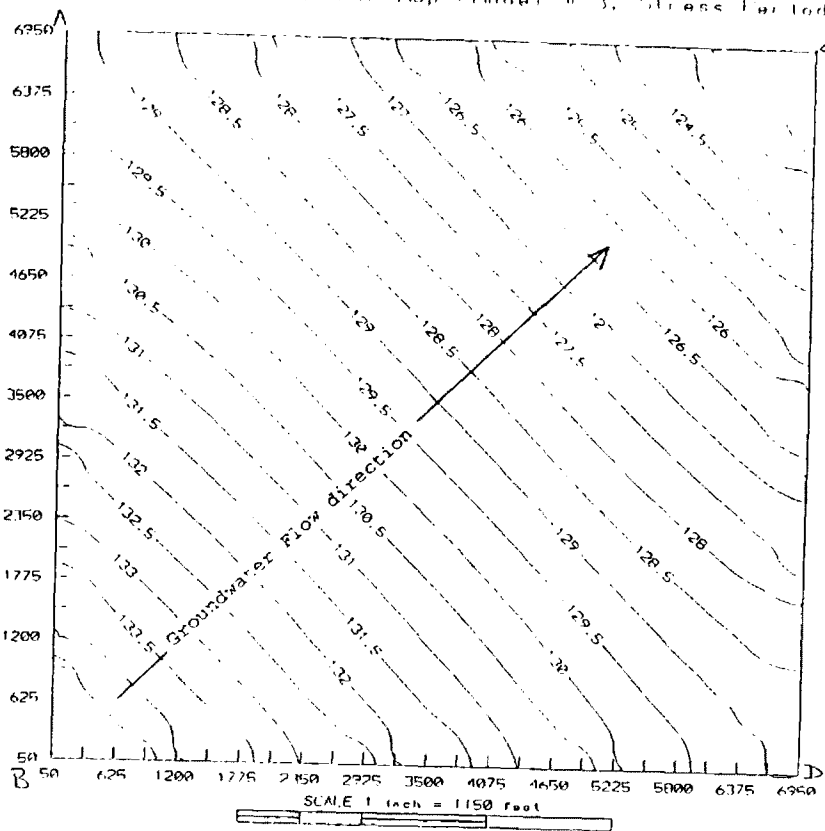


Figure 17. Potentiometric Map (Model # 3, Stress Period 4)

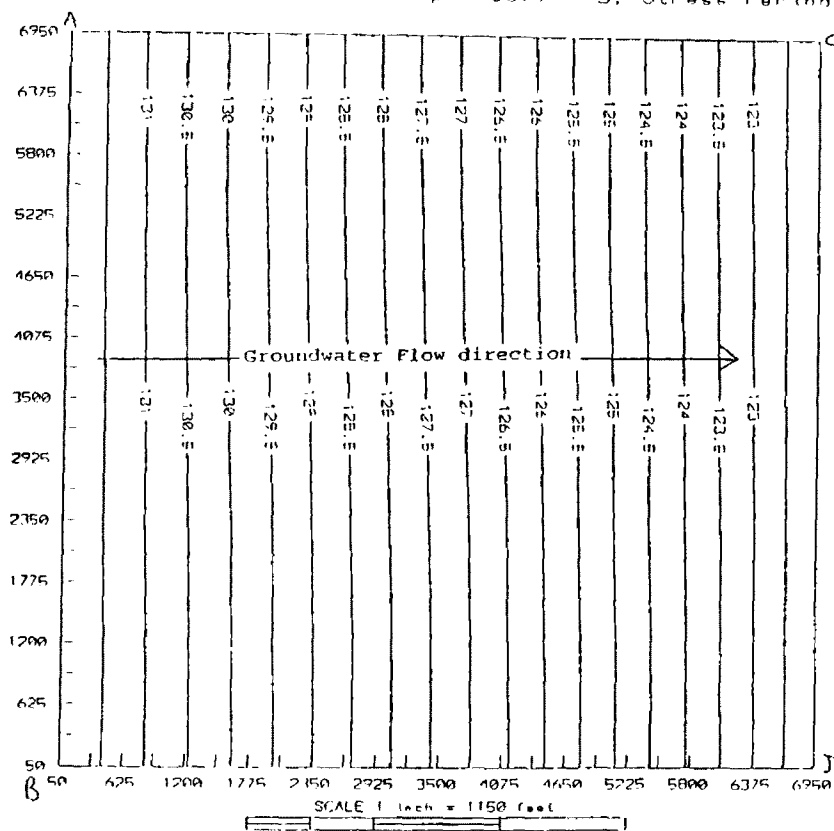
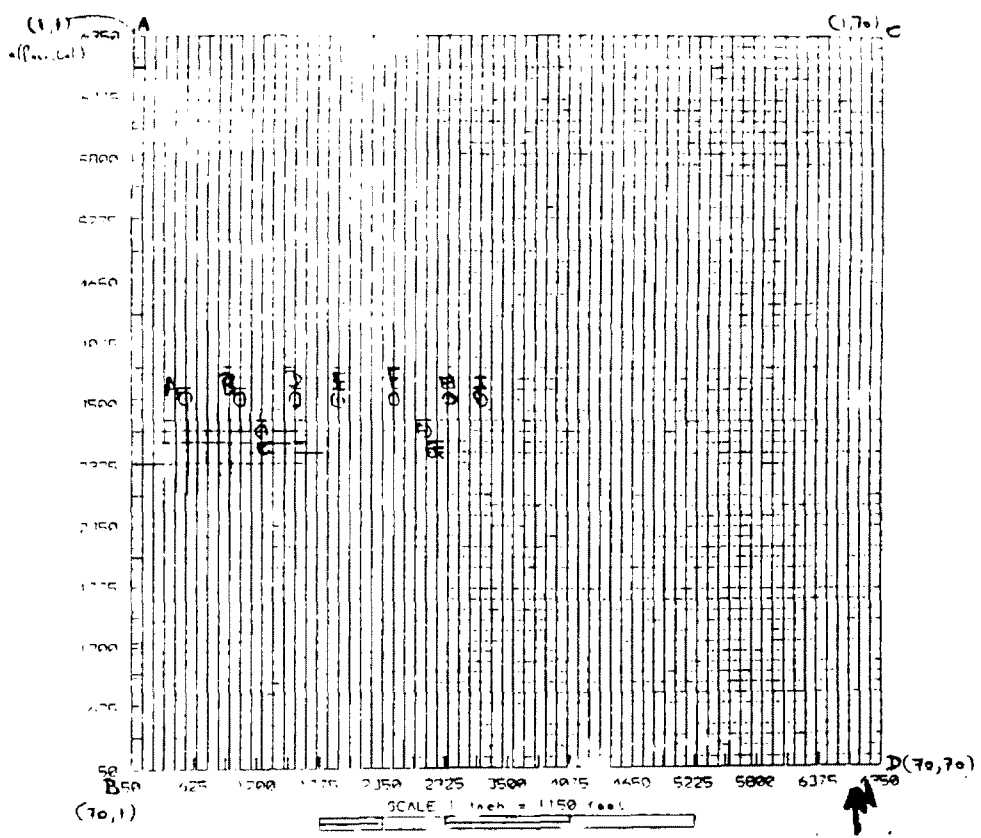


Figure 18. Apparent (X_a) and True X_a flowpaths



A-B-D-E-F-H-I Apparent flowpath
 A-B-C-D-E-F-G-H-I True Flowpath

4.0 RESULTS AND DISCUSSION

The results of each model shows the plume maps with their configurations, breakthrough curves for each plume, and a table summarizing the calculated values of longitudinal dispersivity. A discussion of the results, goes with the presentation.

Figure 19 is a set of dimensionless time versus concentration curves developed from Sauty (1980) for a one dimensional analysis of longitudinal dispersion.

4.1 MODEL # 1

Figures 20 & 21 are maps of the plumes at one and two years. Figures 22 to 26 are the breakthrough curves at point of observation including at one and two years. Table 1 provides a summary of the calculated longitudinal dispersivity values. The first model did not give any conclusive results and the analytically derived results did not match with the model input value of 10 feet for longitudinal dispersivity. This was due to poor discretization of this model grid and not having aligned the grid along the direction of flow of groundwater. The above sequence of presenting the data is repeated for Model # 2 & 3.

4.2 MODEL # 2

Figures 27 to 32 are three sets of plume maps for one and two years for each of the three different scenarios under

Model # 2. Figures 33 to 38 are three sets of breakthrough curves for each of the three sets of plume maps above. Table 2 provides a summary of values of longitudinal dispersivity for each of three scenarios in the model. On comparing the longitudinal dispersivity values from the three scenarios we can see that all the values of longitudinal dispersivity agree very closely with each other, and with the model input value which was 10 feet, except, in the final scenario where longitudinal dispersivity value is 40 feet for the second year location.

In the **first scenario**, the hydraulic conductivity and porosity were held constant. This resulted in one constant velocity field throughout the model. The grid was aligned with the groundwater flow direction. Also, the grid was more finely discretized than in Model # 1. The analytically derived value of longitudinal dispersivity agreed very closely with the modeled value, as the calculations were straight forward in this case.

In the **second scenario**, the hydraulic conductivity was made to vary within the model. The porosity was a constant value of 0.2 throughout the model. As the flux remained constant in and out of the model, the flow simulated hydraulic gradients for each of the constant hydraulic conductivity zones. This resulted in a constant velocity that was less than of the first scenario. Here too the analytically derived value of longitudinal dispersivity agreed very well with the

modelled value and with the values in the first scenario as seen in Table 2.

Also notice, that though the values of longitudinal dispersivity agree well in both scenarios when compared, the distance covered by the plumes, for one and two years in the first scenario, is more than that covered by the plumes in the second scenario as expected.

In the **third scenario**, hydraulic gradients were set up within the model, by using constant head boundaries and aligned perpendicular to the direction of flow. The hydraulic conductivity was kept a constant ($K=700$ ft/d) through the model. The porosity was a constant of 0.2 . This varied the velocity systematically within the model.

It can be seen from Table 3, that the location of the first year longitudinal dispersivity value agrees well with the modelled value of 10 feet and, with the first and second scenarios results. But, the second year location of the plume, shows a value of longitudinal dispersivity that is very high (40 feet), and does not agree with the modelled value of 10 feet. This value of longitudinal dispersivity is also in disagreement with the first two scenarios.

Typically under isotropic homogeneous conditions values of transverse dispersivity are at least one order of magnitude lower than the longitudinal dispersivity values (Cherry et al., 1975; Goode and Konikow, 1990).

In the paper by Goode and Konikow (1990) they conclude

that unrecognized flow field transients that change the direction of flow of a plume cause an increase in the transverse dispersivity because longitudinal dispersion is acting in a direction that is not parallel to the assumed direction of flow.

Thus, I **hypothesies**, that the high value of longitudinal dispersivity (40 feet) in the third scenario, is due to the constant head boundary within the model that increased the transverse dispersion due to change in gradient and thus velocity of the flow. I believe this to be so as the plume travels from a higher velocity zone to a lower velocity zone. The other explanation could be that the longitudinal dispersion had actually increased as seen in Table 2 which is contrary to my understanding.

4.3 MODEL # 3

I have presented the results of the **transient** Model # 3, in the same format as the other models. Figures 39 to 46 are maps showing the locations and extent of the various plumes in time (including one and two years). Figures 47 to 54 are breakthrough curves associated with the above plumes. Table 3 provides a summary of the calculated longitudinal dispersivity values.

It can be seen from Table 3, that values calculated from the data close to the point of injection are lower than values calculated from data recorded at larger distances. Also, the

value of **true longitudinal dispersivity** measured along the true flowpath (X_t) are **higher** than the **apparent longitudinal dispersivity** values measured along a straight line or apparent flowpath (X_a).

In the paper by Goode and Konikow (1990) they conclude that unrecognised flow field transients that change the direction of flow of a plume cause an increase in the transverse dispersivity because longitudinal dispersion is acting in a direction that is not parallel to the assumed direction of flow.

Thus, Model # 2 & 3 indicate that field derived values of longitudinal dispersion should be increased to account for flow field transients such as minor and major fluctuations in velocity and flowpath.

Figure 19. Type Curves for Selected Peclet Numbers

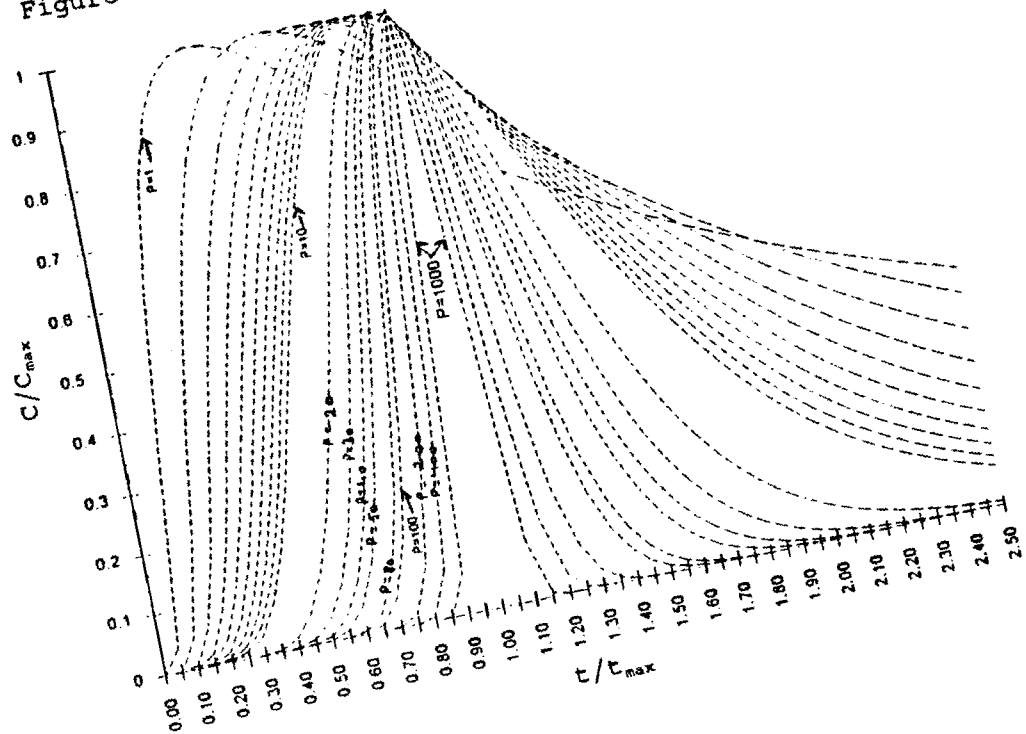


Figure 22. Plume Map (Model #1, 1 year)

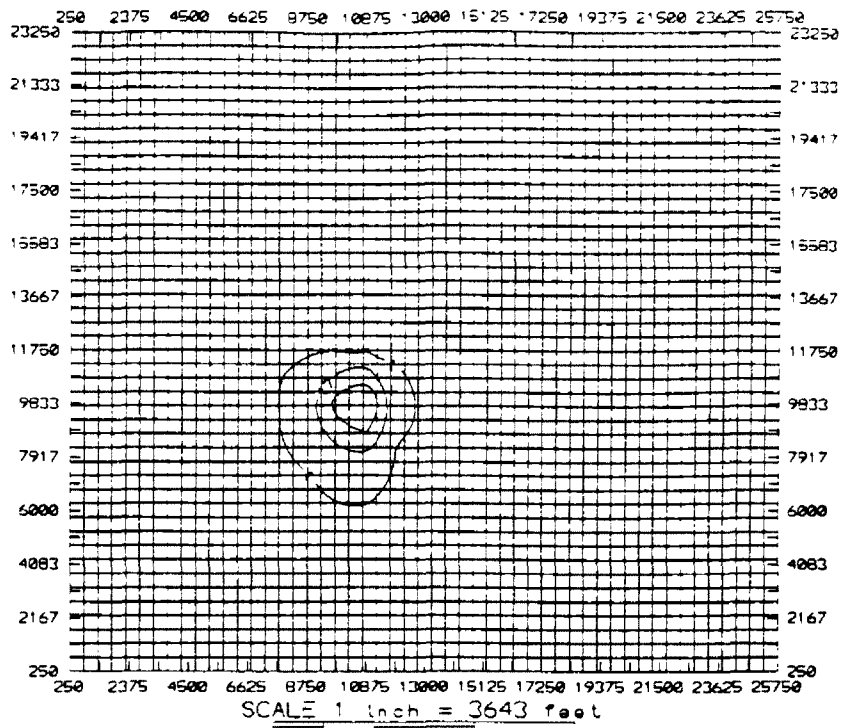


Figure 21. Plume Map (Model #1, 2 years)

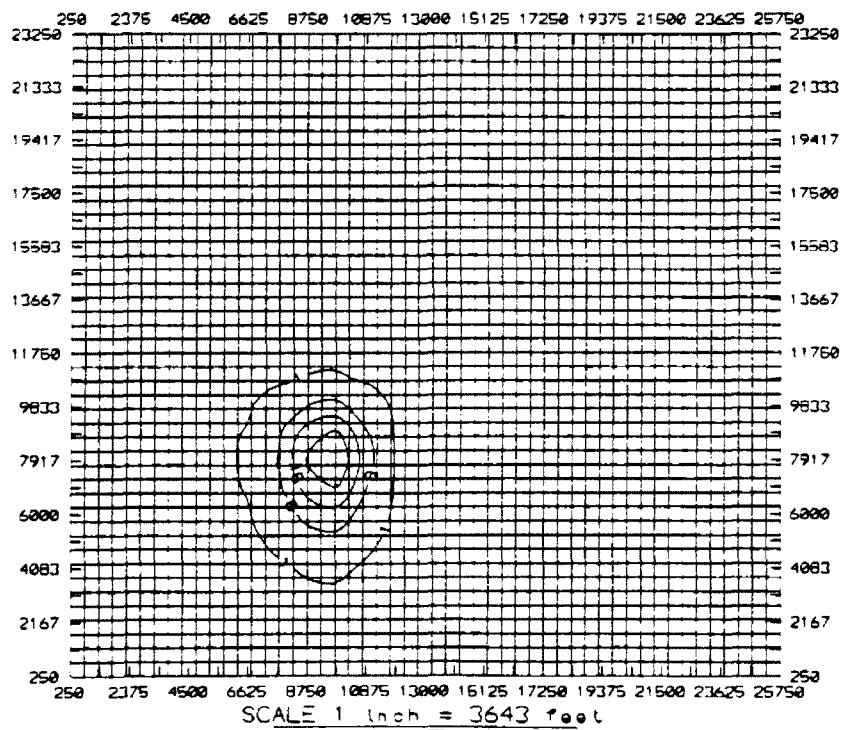


Figure 22 (row, col)=(26, 22). Model # 1

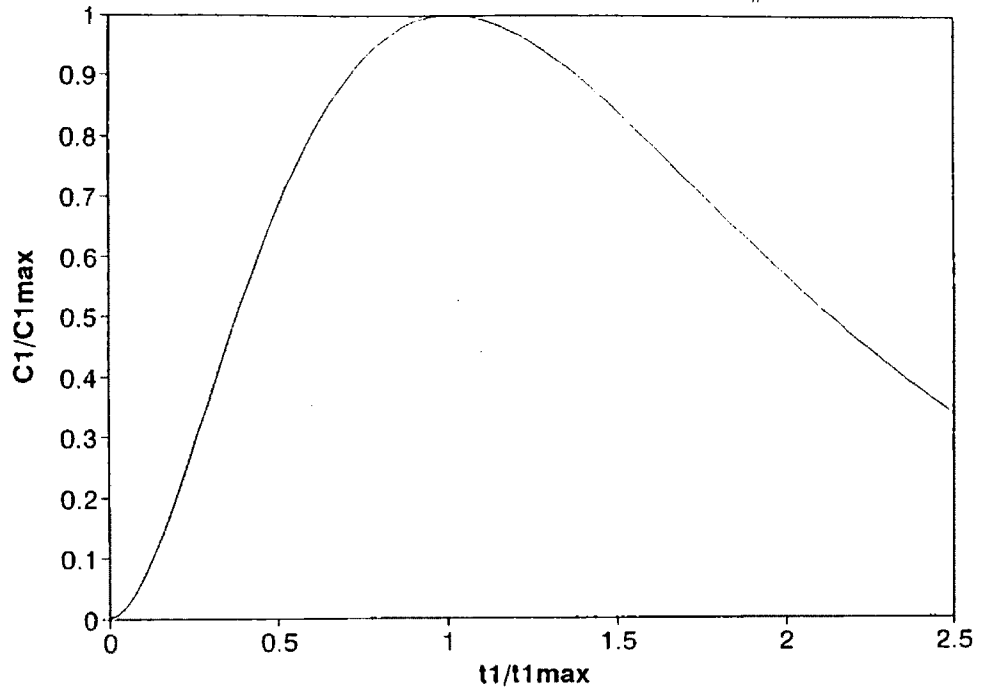


Figure 23 (row, col)=(27, 22) Model # 1

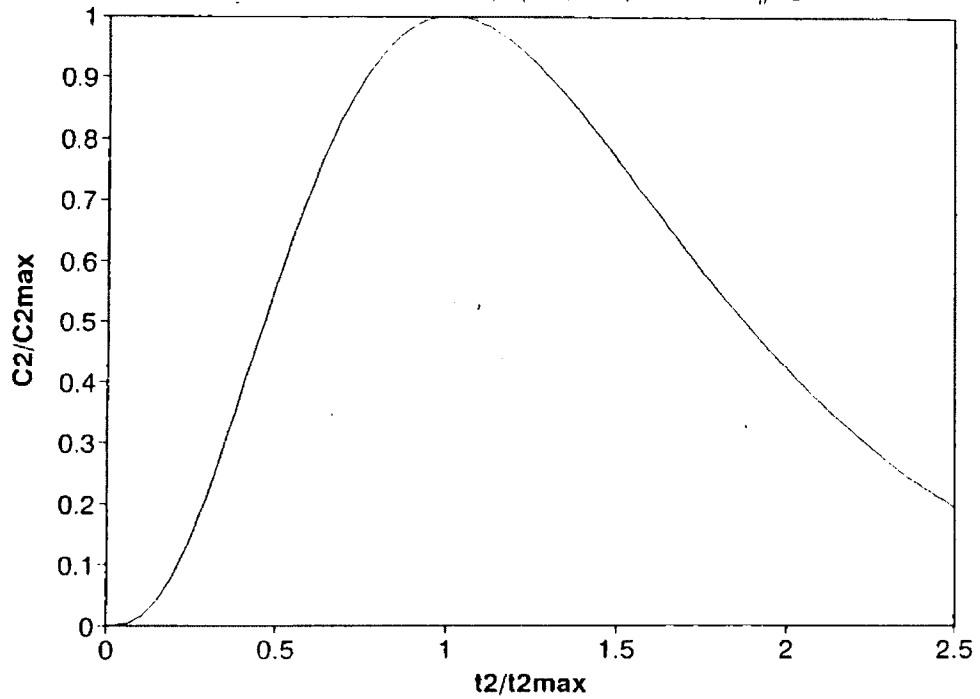


Figure 24 (row, col)=(28, 21) Model # 1

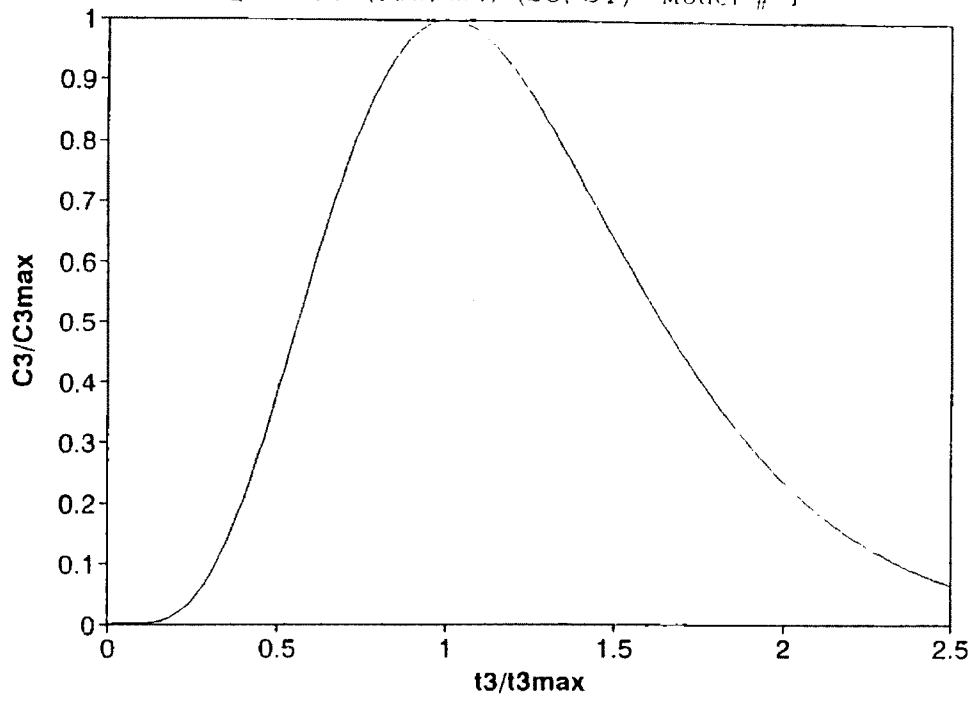


Figure 25 (row, col)=(29, 21) Model # 1

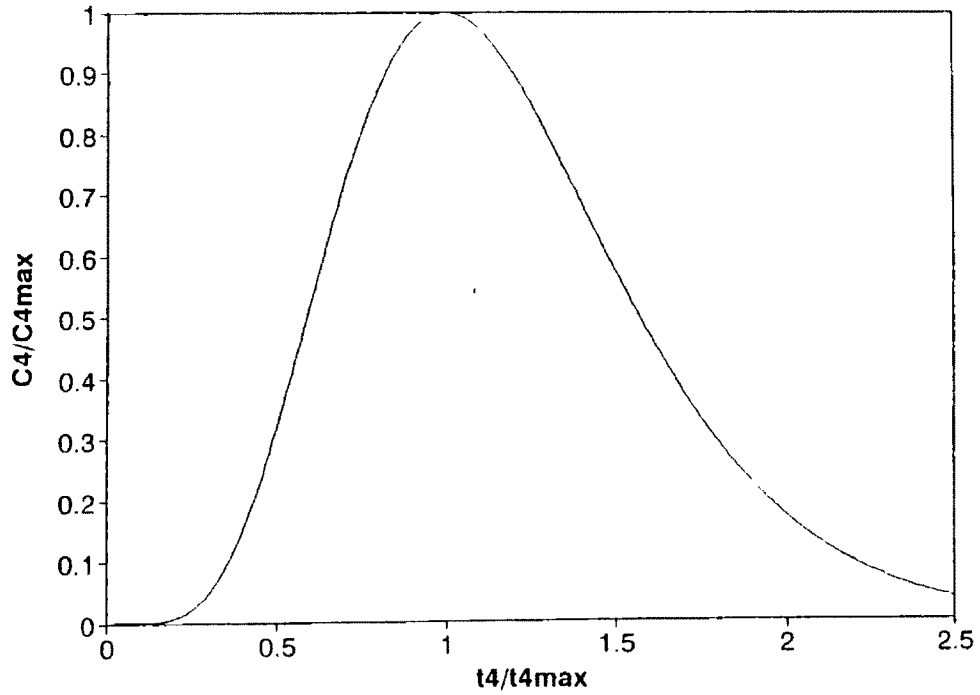


Figure 26 (row, col)-(32, 20) Model # 1

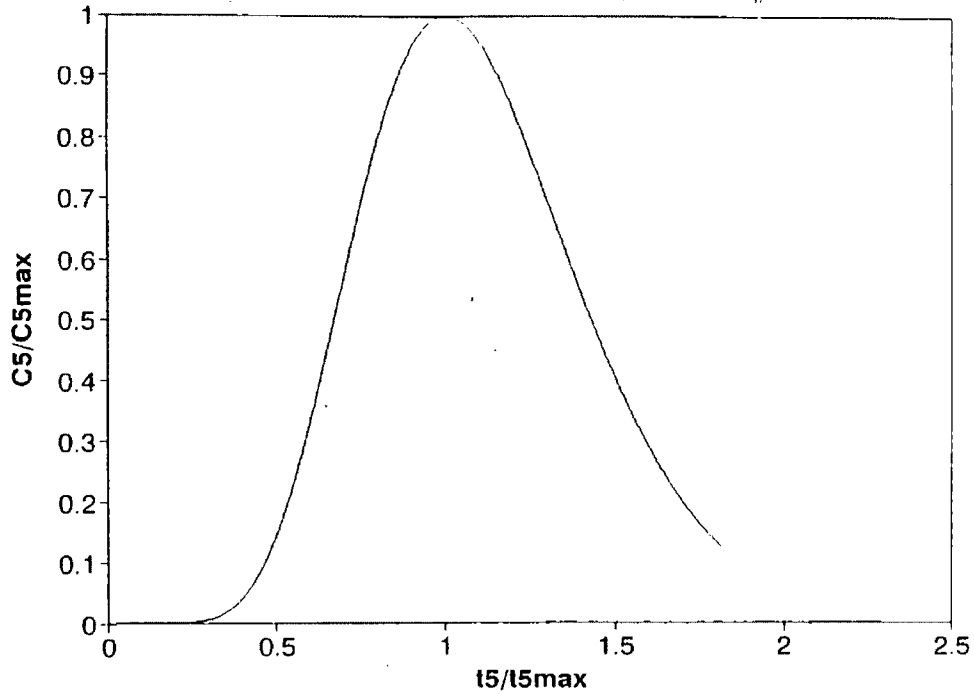


TABLE 1.

Summary of calculated longitudinal dispersivity values (Model # 1)

{layer,row,column}	X	P	Long.Disp. = X / P
	(feet)		(feet)
{1,25,23} input			
{1,26,22}	707	2	353
{1,27,22}	1207	5	241
{1,28,21}	1914	9	212
{1,29,21} 1 yr.	2414	13	185.6
{1,32,20} 2 yrs.	3532	20	176.6

X = Distance travelled by centre of plume

P = Peclet number retrieved from curve matching

{layer,row,column} = points of observation

Figure 27. Plume Map (Model #2, First Scenario, 1 year)

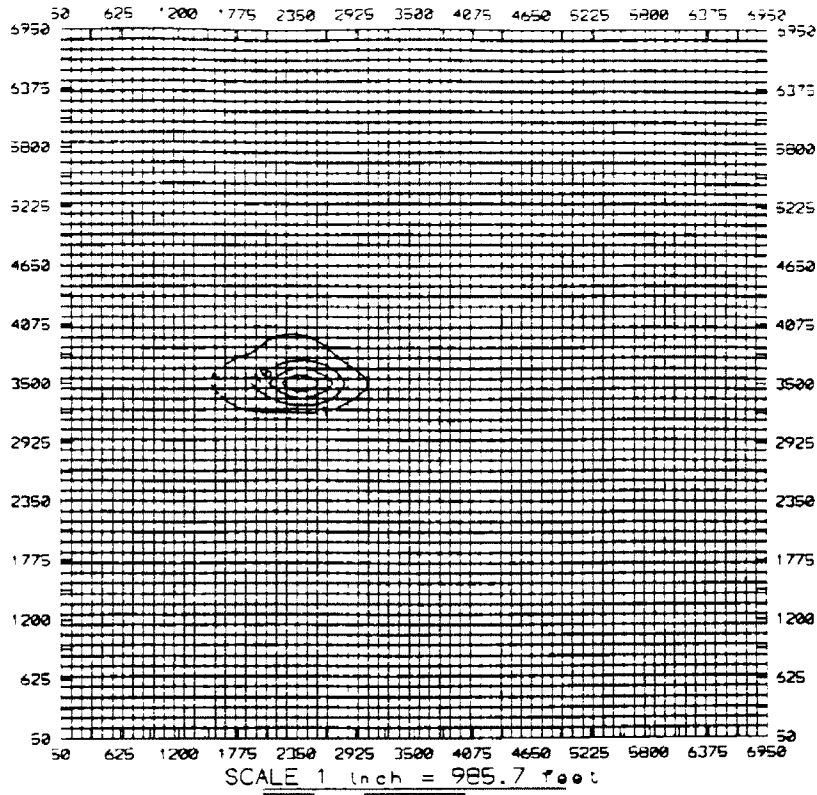
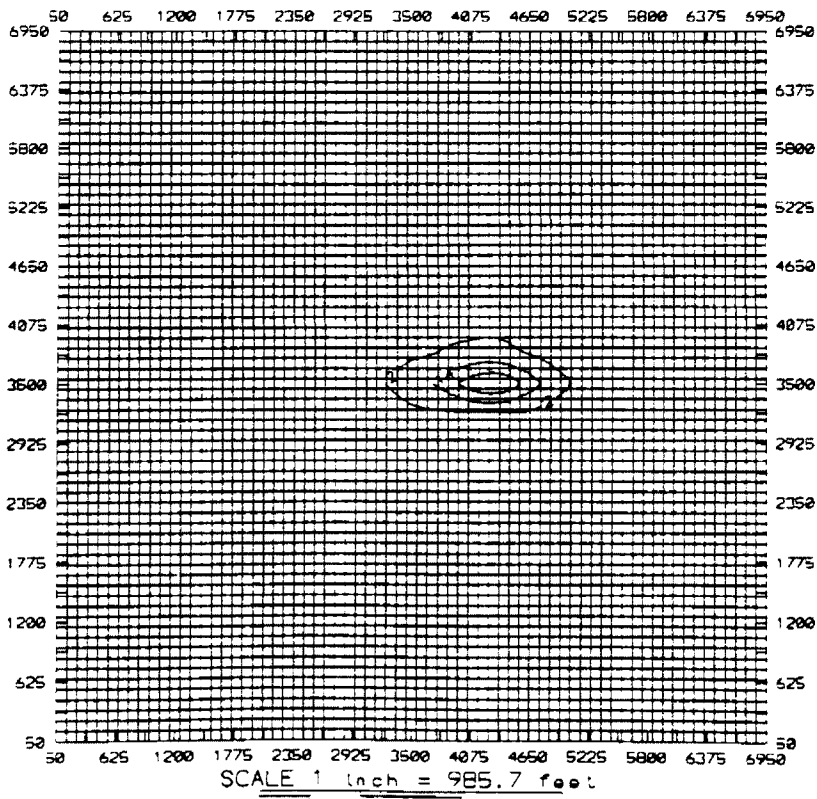


Figure 28. Plume Map (Model #2, First Scenario, 2 years)



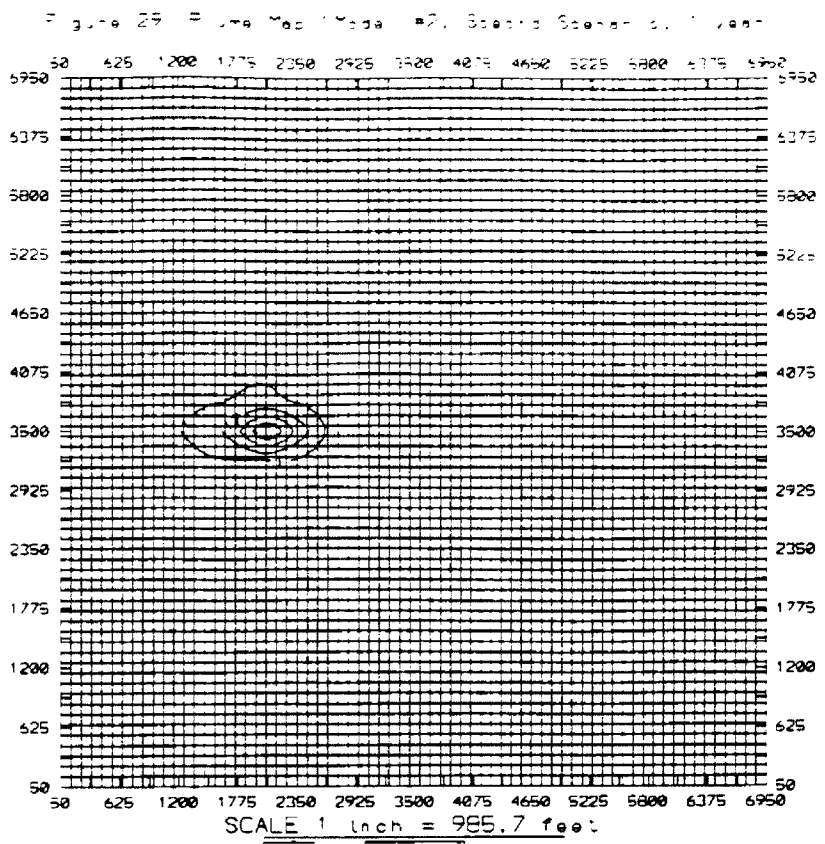


Figure 30. Plume Map (Model #2, Second Scenario, 2 years)

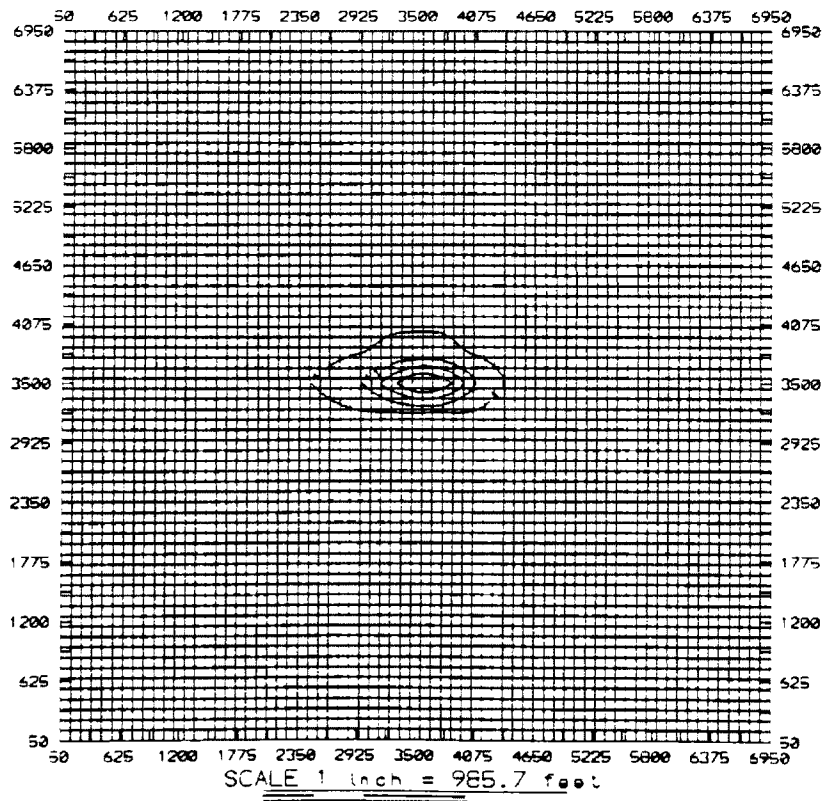


Figure 31. Plume Map (Model #2, Third Scenario, 1 year)

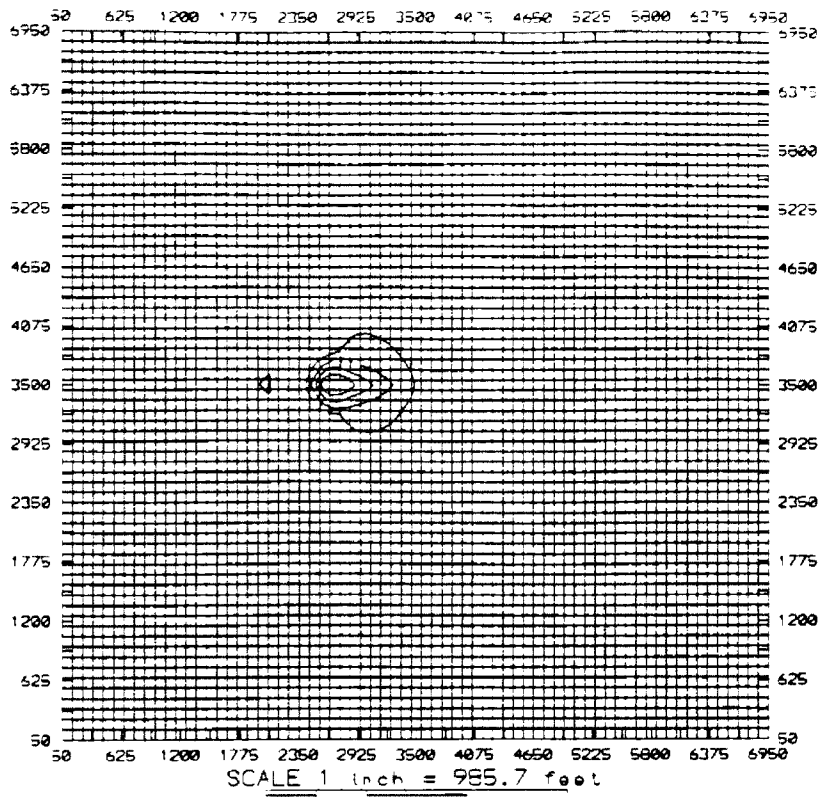


Figure 32. Plume Map (Model #2, Third Scenario, 2 years)

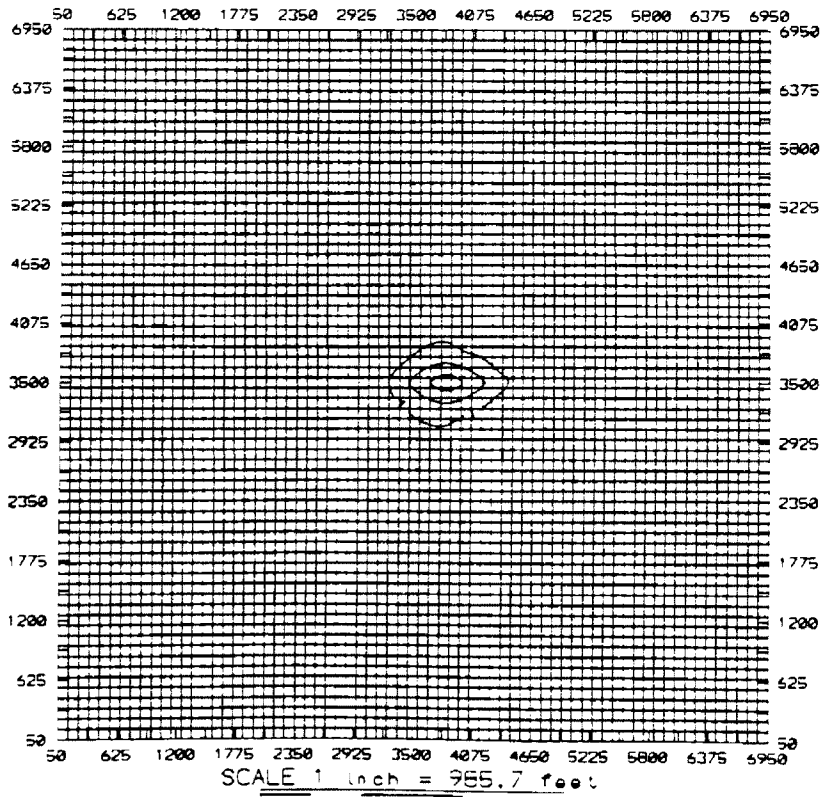


Figure 33 (row, col)=(35, 25) Model # 2 First Scenario

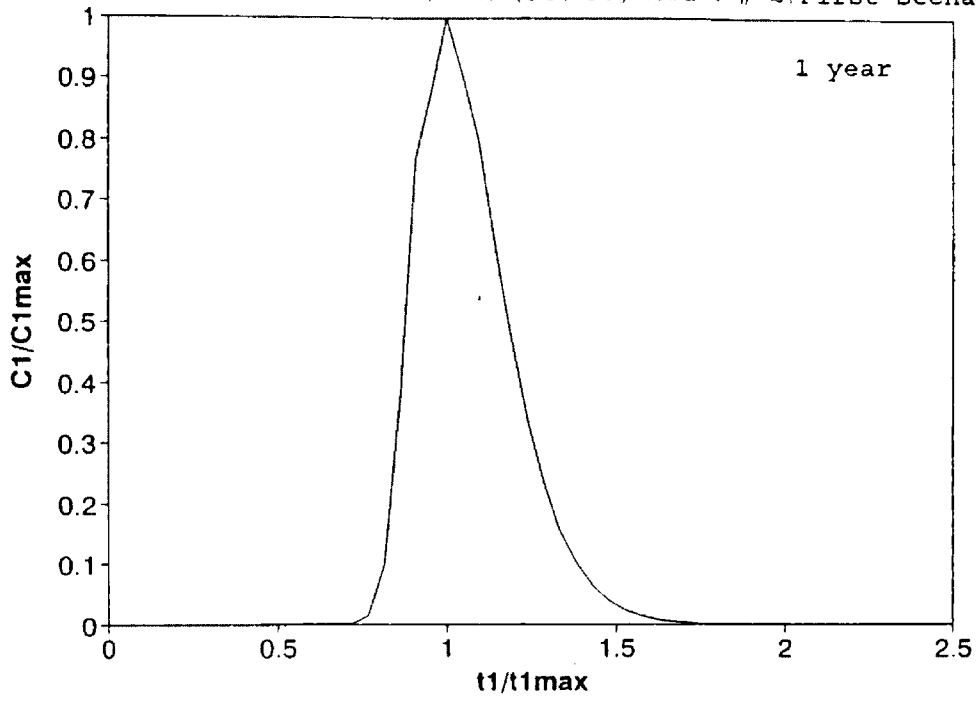


Figure 34 (row, col)=(35, 43) Model # 2 First Scenario

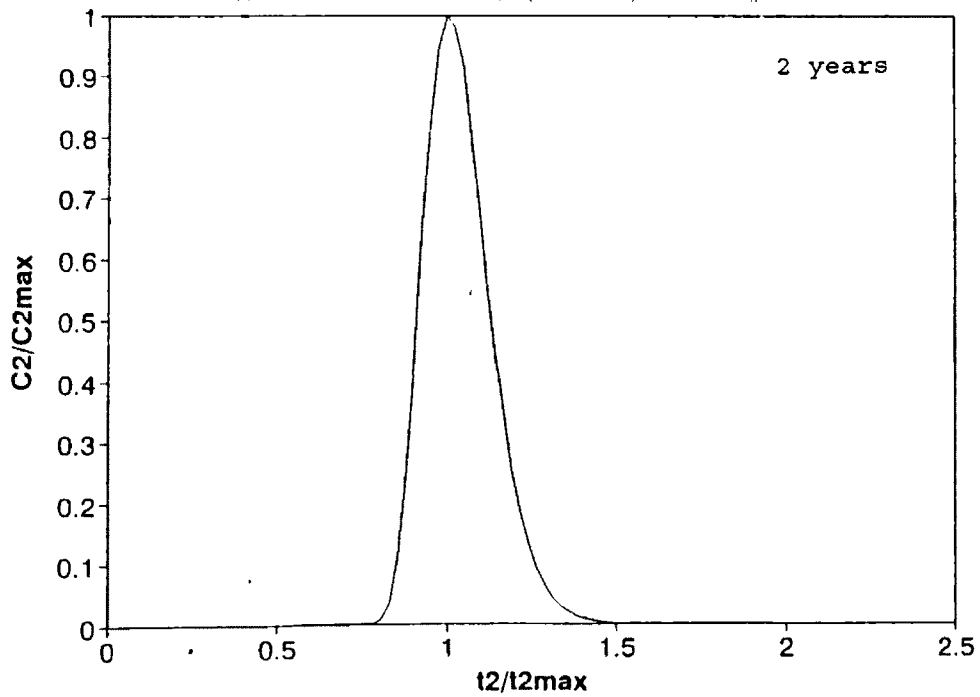


Figure 35 (row, col)=(35, 21) Model # 2 Second Scenario

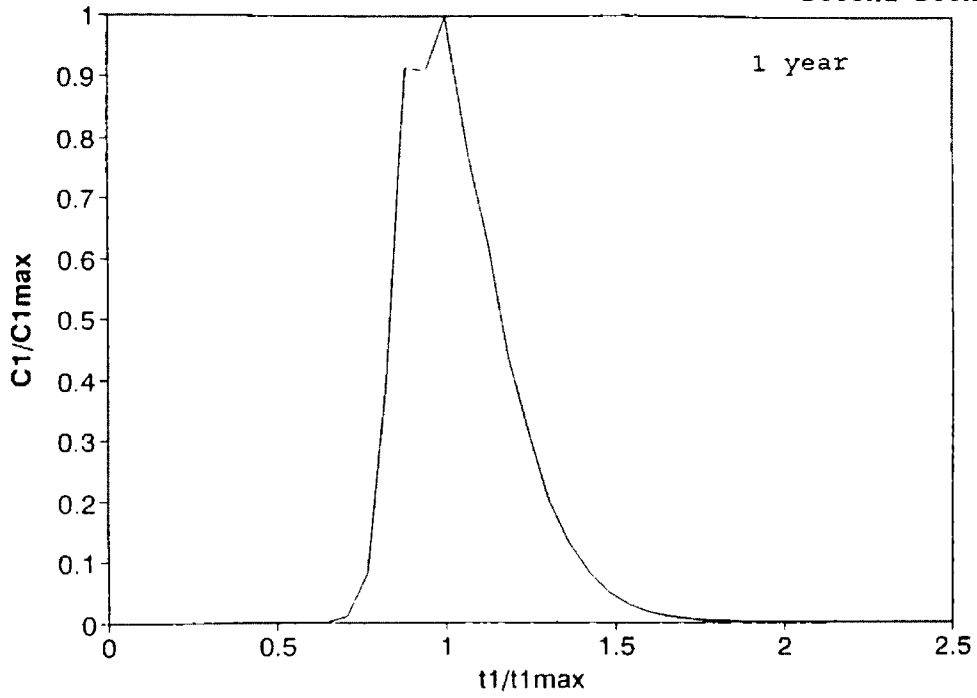


Figure 36 (row, col)=(35, 36) Model # 2 Second Scenario

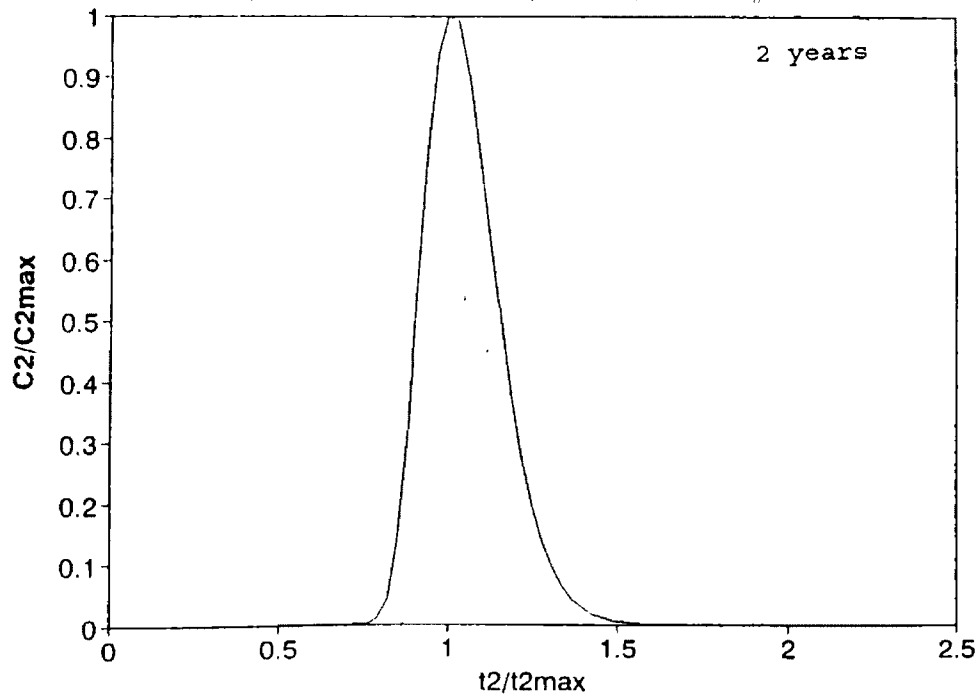


Figure 37 (row, col)=(35, 28) Model # 2 Third Scenario

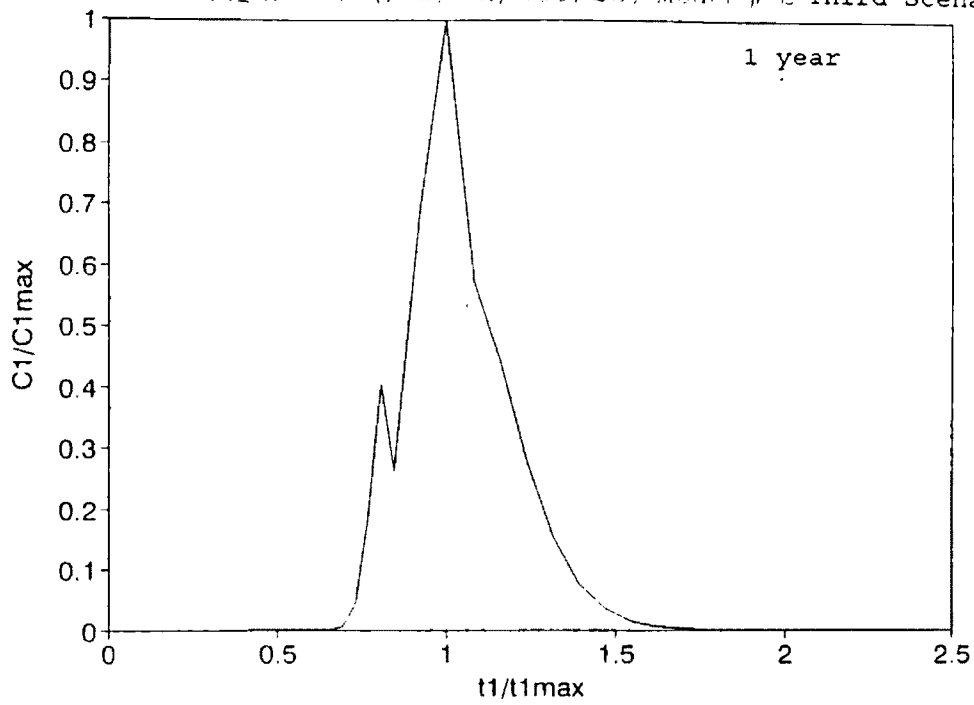


Figure 38 (row, col)=(35, 38) Model # 2 Third Scenario

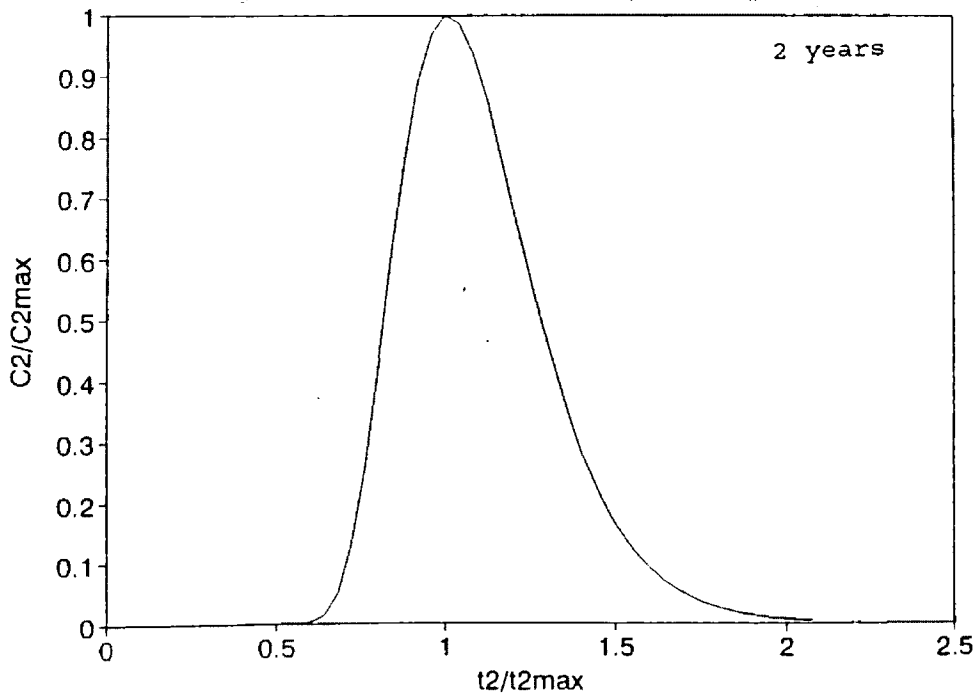


TABLE 2
Summary of calculated longitudinal dispersivity values (Model # 2)

{layer,row,column}	X (feet)	P	Long.Disp. = X / P (feet)
{1,35,6} input			
First scenario			
{1,35,25} 1 yr.	1900	200	9.5
{1,35,43} 2 yrs.	3700	350	10.6
Second scenario			
{1,35,21} 1 yr.	1500	150	10
{1,35,36} 2 yrs.	3000	300	10
Third scenario			
{1,35,28} 1 yr.	2200	200	11
{1,35,38} 2 yrs.	3200	80	40

X = Distance travelled by centre of plume

P = Peclet number retrieved from curve matching

{layer,row,column} = points of observation

Figure 39. Plume Map (Model #2, 91 days)

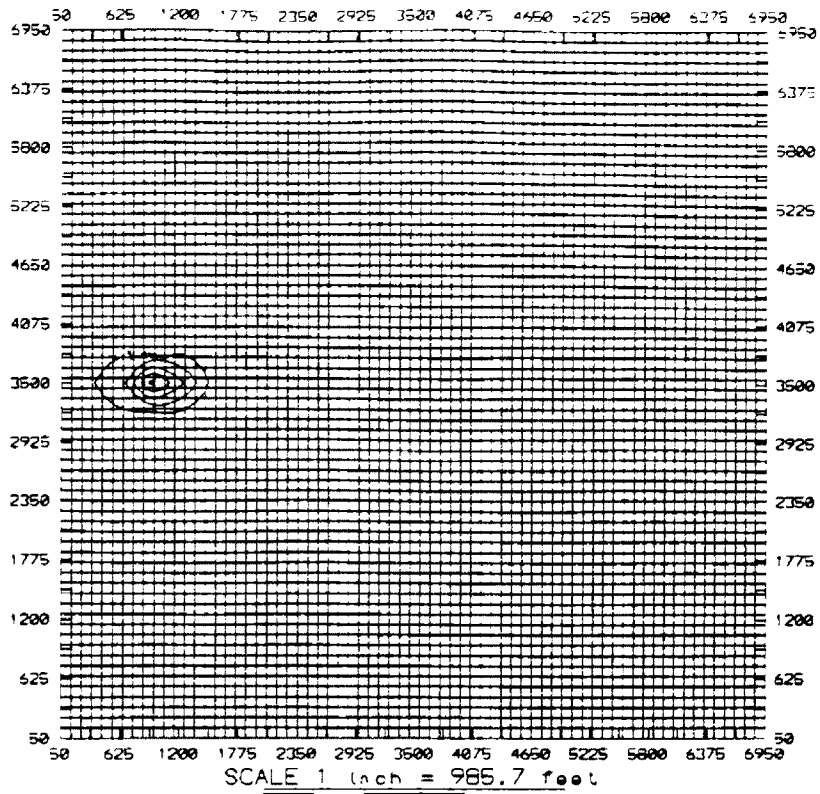


Figure 40. Plume Map (Model #3, 182 days)

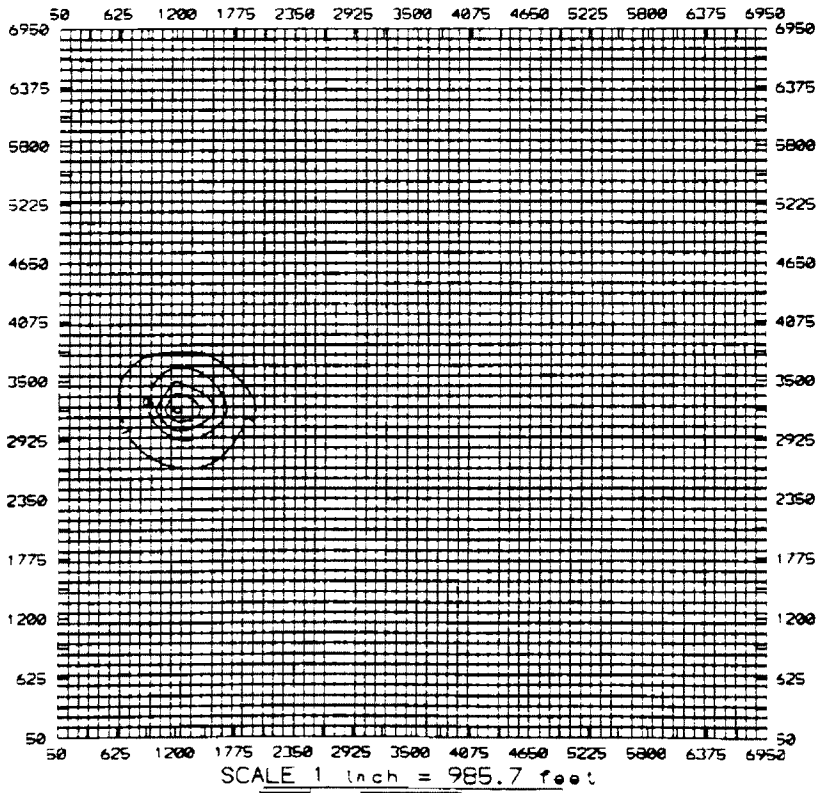


Figure 41. Plume Map (Model #1, 365 days)

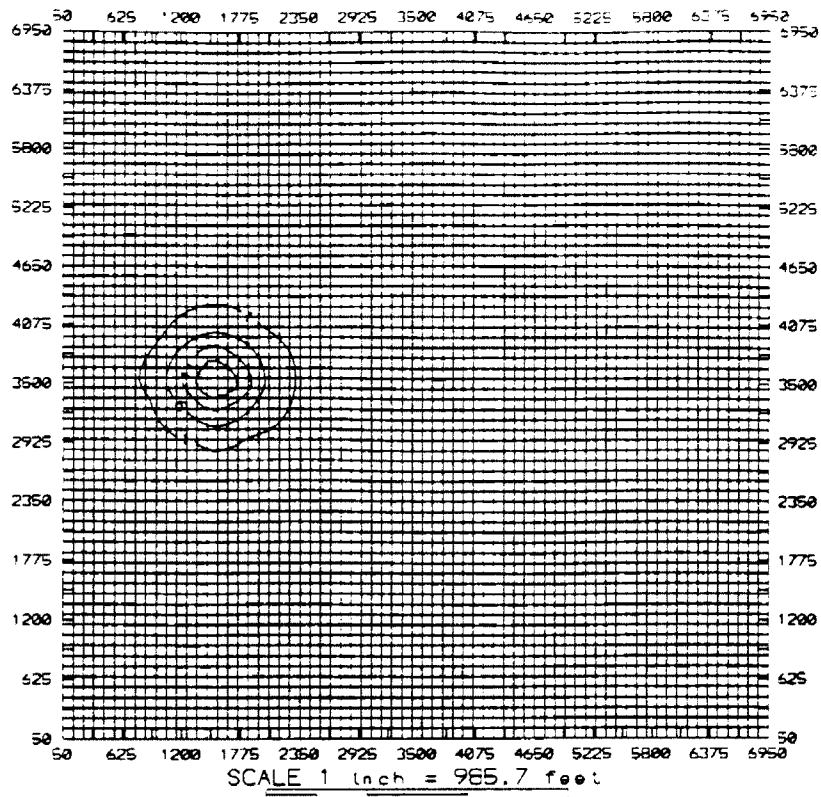


Figure 42. Plume map (Model #3, 365 days)

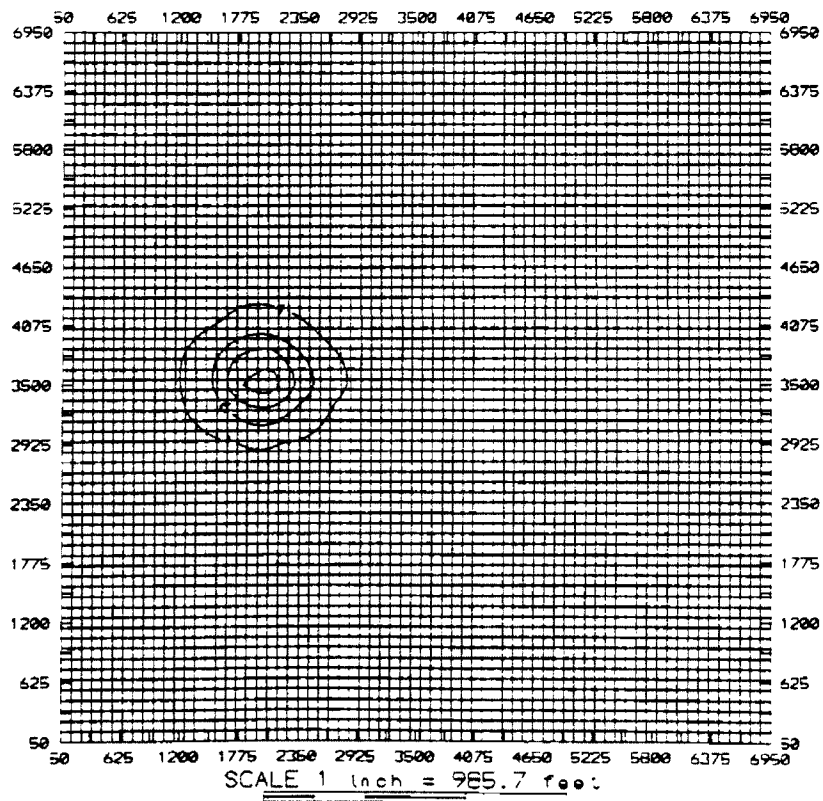


Figure 43. Plume map (Model #3, 456 days)

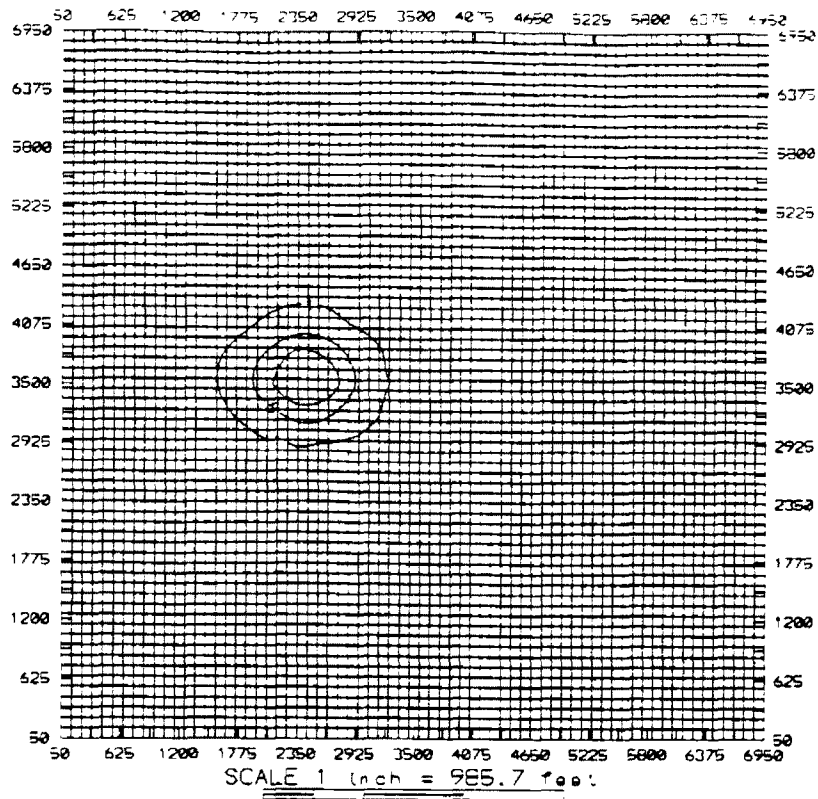


Figure 44. Plume map (Model #3, 547 days)

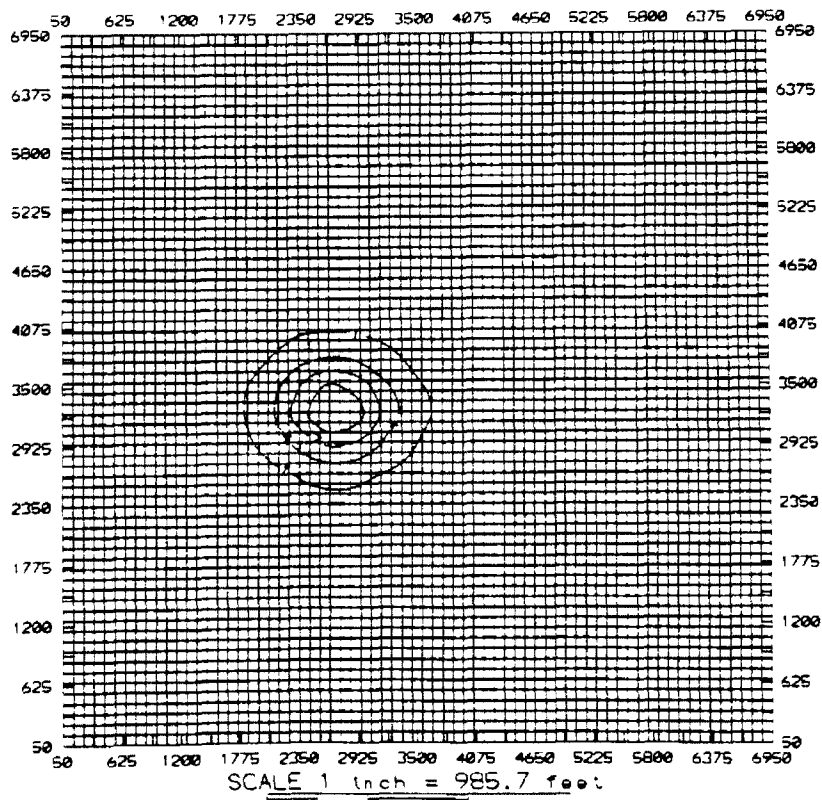


Figure 45. Plume map (Model #0, 638 days)

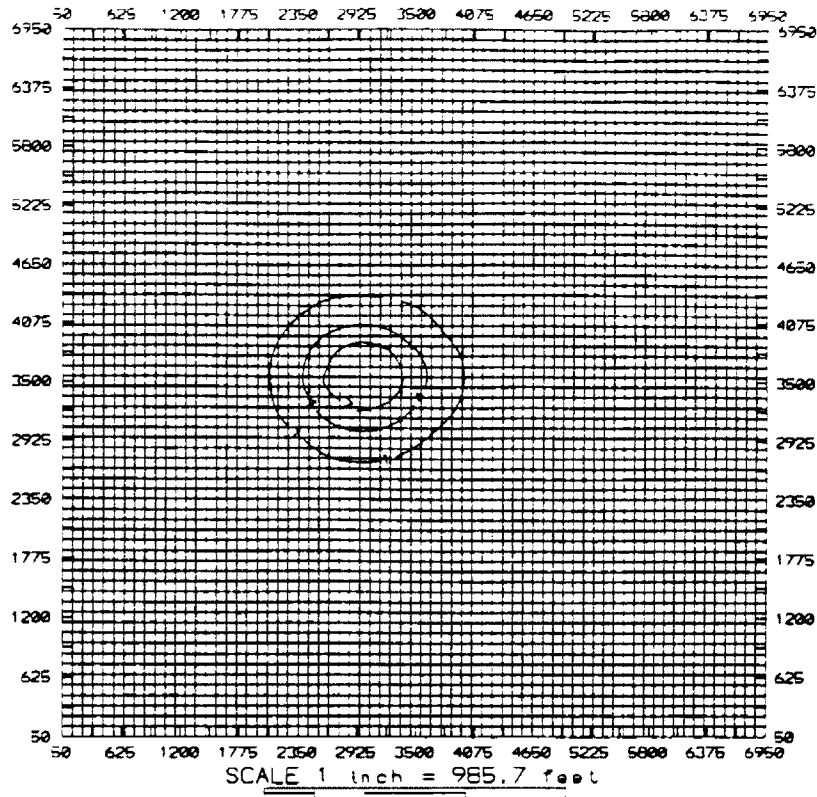


Figure 46. Plume Map (Model #3, 730 days)

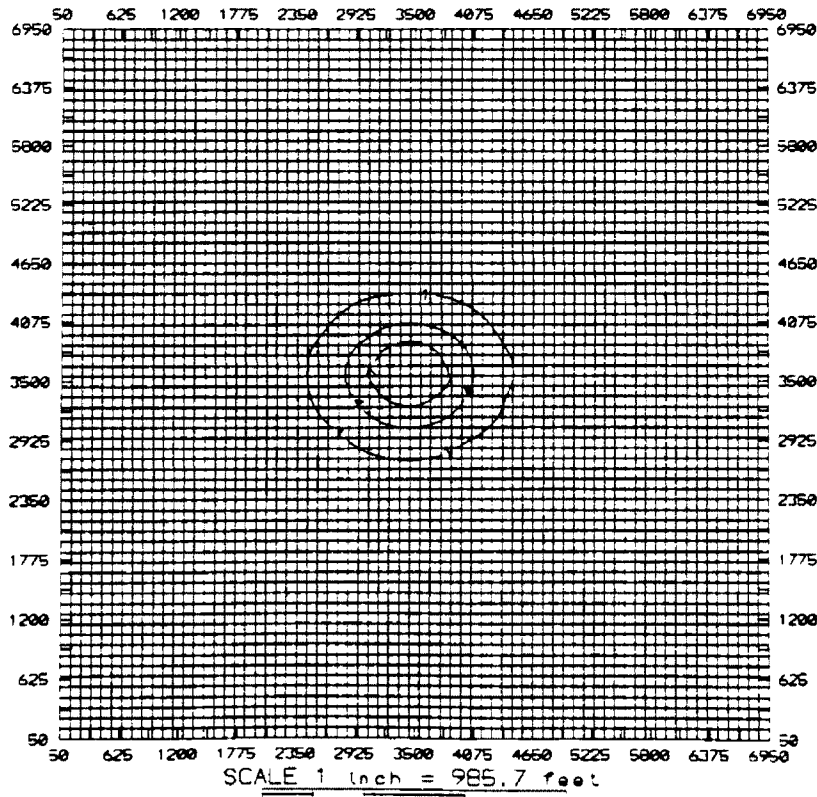


Figure 47 (row, col)=(35, 11) Model # 3

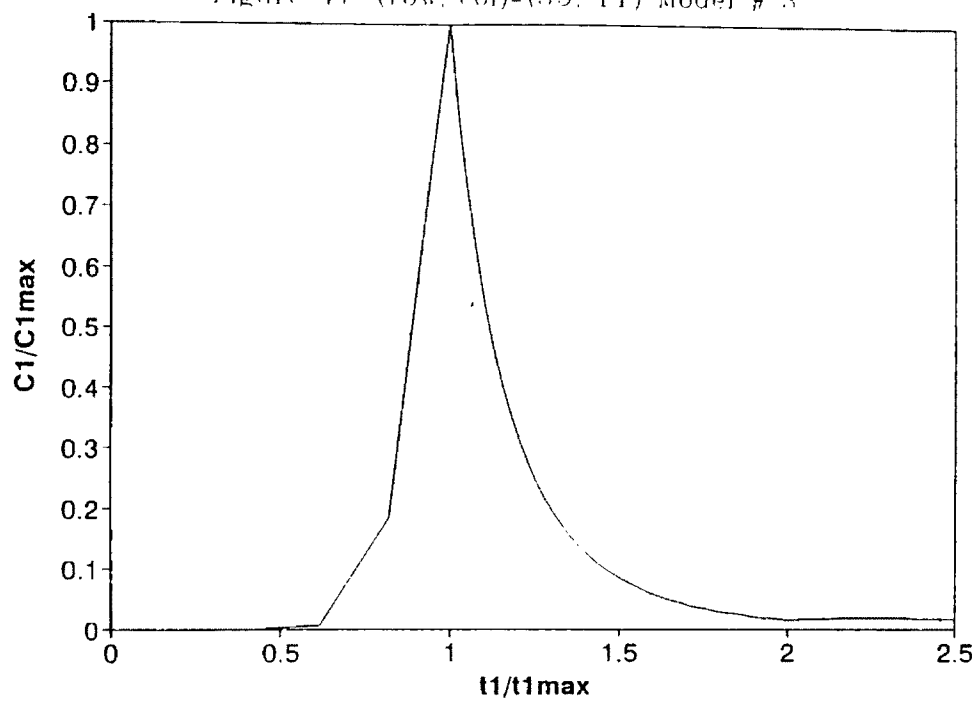


Figure 48 (row, col)=(38, 13) Model # 3

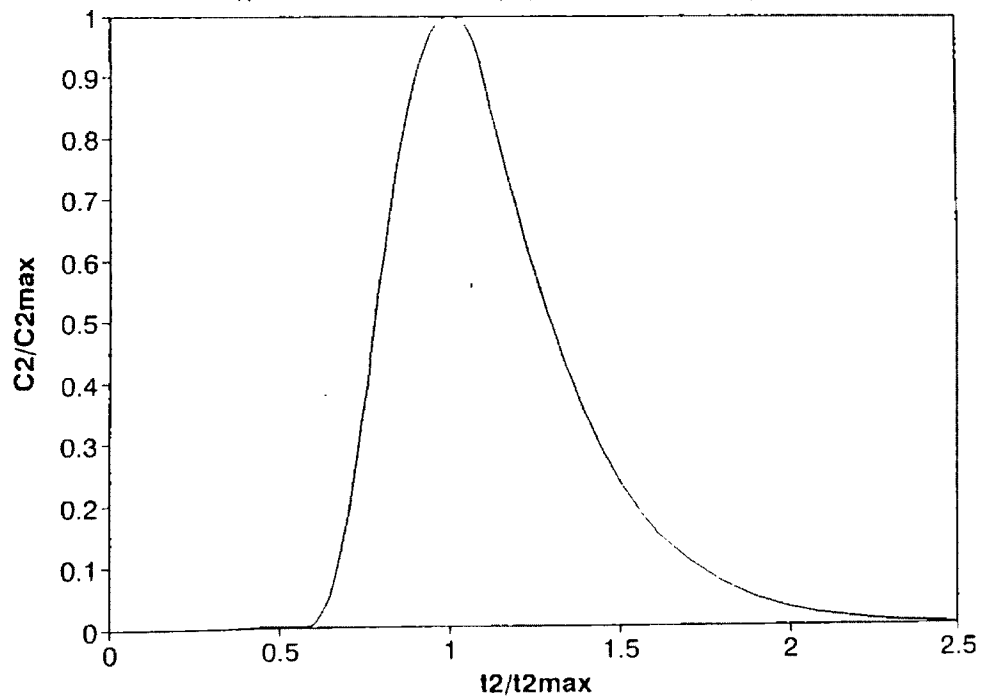


Figure 19 (row, col) = (35, 16) Model # 3

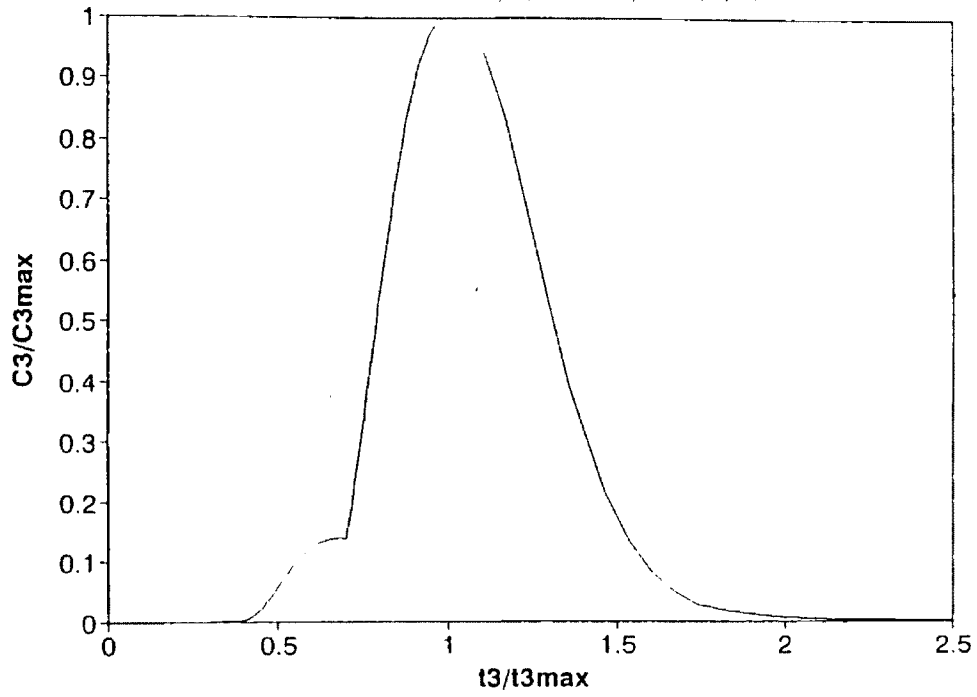


Figure 50 (row, col) = (35, 20) Model # 3

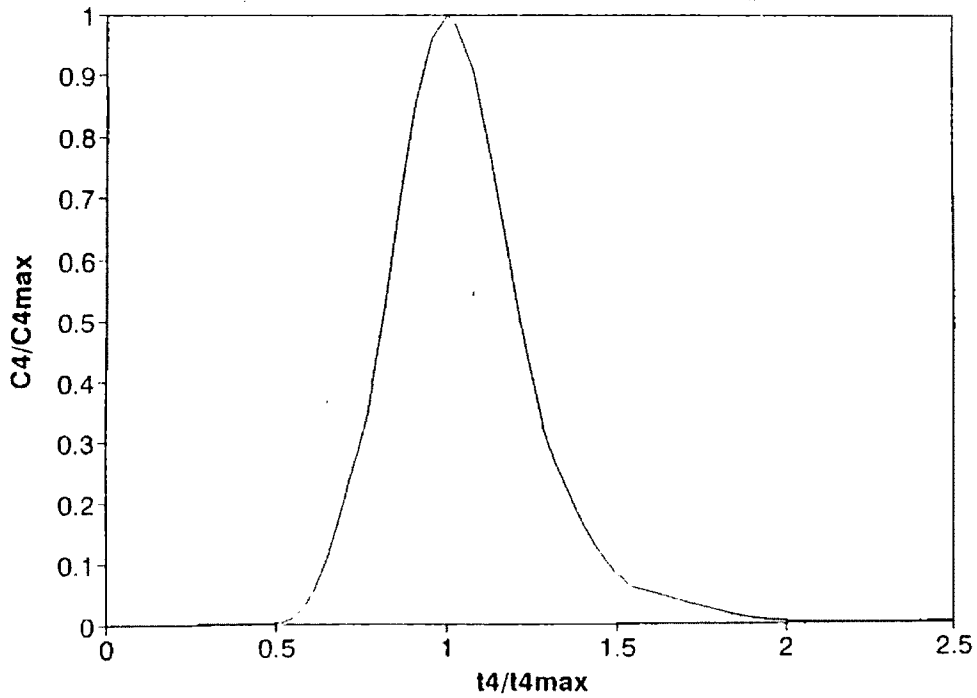


Figure 51 (row, col)=(35, 25) Model # 3

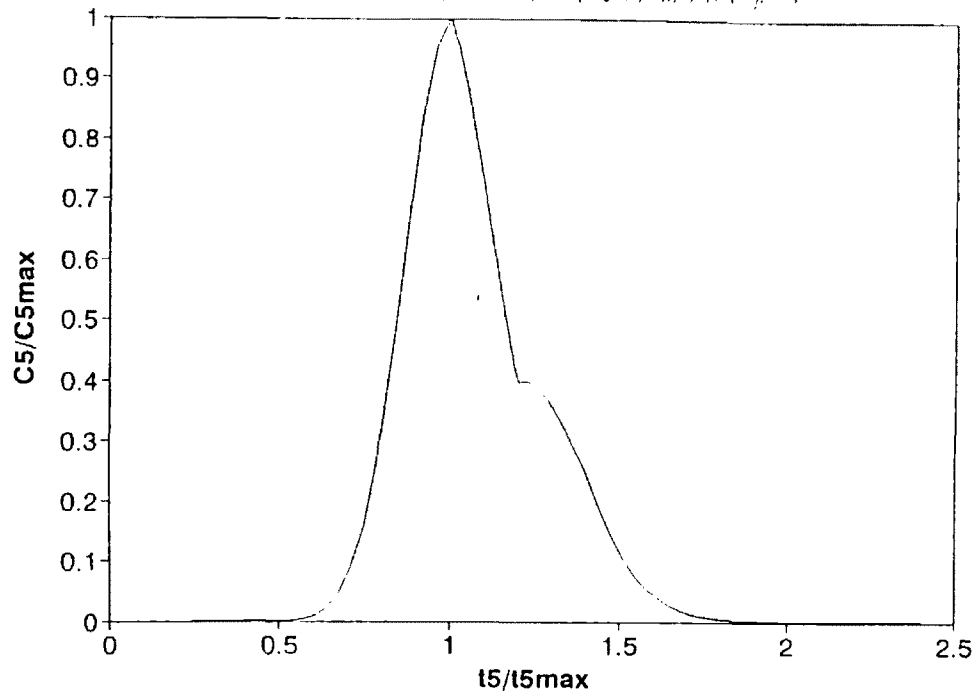


Figure 52 (row, col)=(38, 28) Model # 3

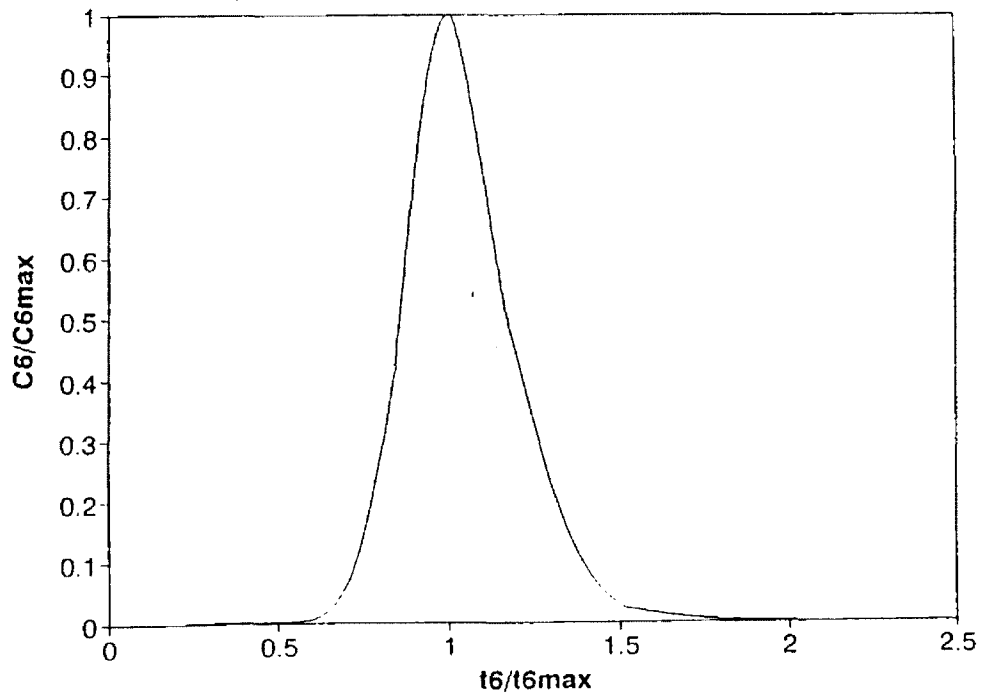


Figure 53 (row, col)=(35, 30) Model # 3

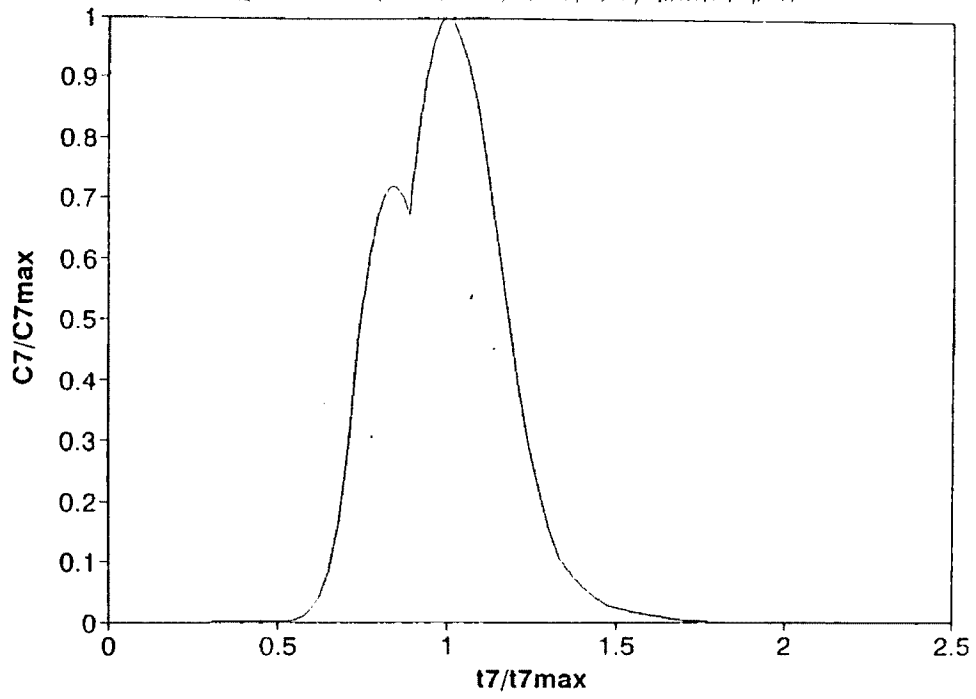


Figure 54 (row, col)=(35, 33) Model # 3

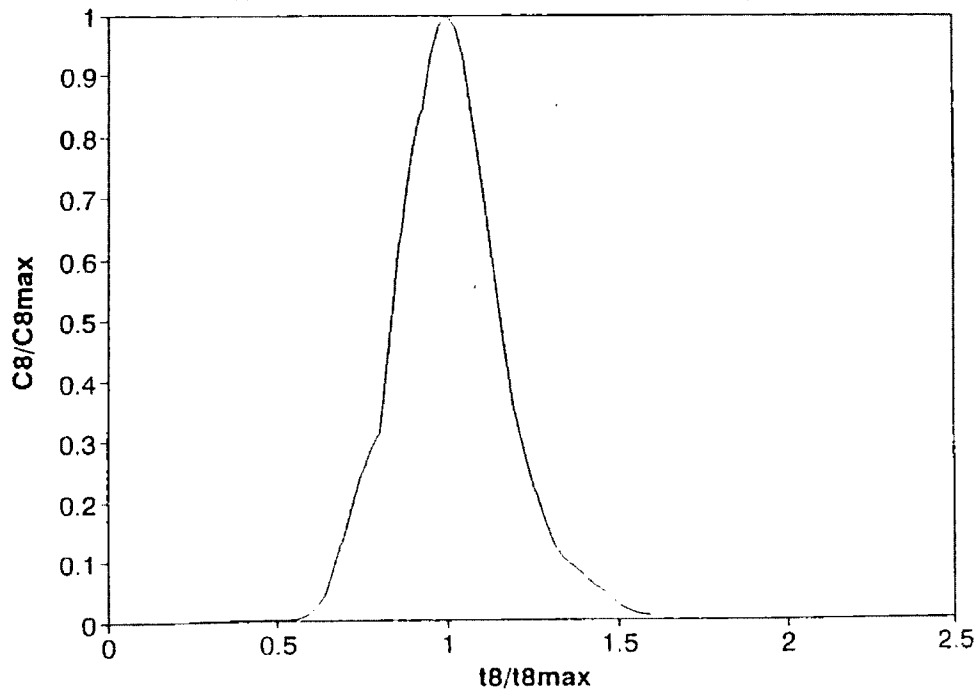


TABLE 3
 Summary of calculated longitudinal dispersivity values (model #3)
 True and Apparent Longitudinal Dispersivity values are shown.

{layer,row,column}	Xt (feet)	Xa (feet)	P	Long.Disp. = Xt / P (feet)	Long.Disp. = Xa/P (feet)
{1,35,6} input					
{1,35,11}	500		200	2.5	
{1,38,13}	860		70	12.3	
{1,35,16}	1284	1000	70	18.3	14.3
{1,35,20} 1 yr.	1684	1400	80	21	17.5
{1,35,25}	2184	1900	100	21.8	19
{1,38,28}	2608		100	26	
{1,35,30}	2968	2400	150	19.7	16
{1,35,33} 2 yrs.	3268	2700	150	21.8	18

Xt = true distance travelled by centre of plume (along varying flowpath)

Xa = apparent distance travelled by centre of plume (straight line path assumed)

P = Peclet number retrieved from curve matching

{layer,row,column} = points of observation

5.0 CONCLUSIONS AND RECOMMENDATIONS

The spreading process is poorly represented when regional scale flow model results are used as input to solute transport codes (not easily reproduced with analytic solutions).

When discretization of the initial field setting into 100 ft. * 100 ft. cells was used and a constant velocity field was created, analytical solutions of modeled plumes for longitudinal dispersivity matched input value.

When the velocity field is varied from 6.0 ft/d to 2.0 ft/d as in model # 2, scenario three, second year position, the plume is spread such that the apparent longitudinal dispersivity increased four times the actual modeled value.

The results of model # 3 indicate that a directionally varying flow field (flowpath variation) with a constant magnitude of velocity, results in an increase in predicted true and apparent longitudinal dispersivity values.

Interestingly, model # 3 also indicates that the value of apparent longitudinal dispersivity (straight line distance) is always less than the true longitudinal dispersivity calculated using actual flowpath length.

Overall, the results indicate that variations in magnitude of groundwater velocity or a directionally varying flowfield within an unconfined aquifer system, can cause an increase in the longitudinal dispersivity of a slug injected contaminant plume. These flow field changes allow for a large portion of the solute to move transversely to the flow

direction, causing more plume dispersion.

I recommend the further research as follows :

- 1) Vary the magnitude of velocity in small increments to determine when the significant changes in longitudinal dispersion occur.
- 2) Vary the distance and angle of flowpath to determine when the significant changes in longitudinal dispersion occur.

REFERENCES

- Ackerer, P. , and W. Kinzelbach, 1985. Modelisation du transport de contaminant par la methode de marche au hasard - Influence des variations du champ d'ecoulement au cours du temps sur la dispersion. Paper presented at the symposium on the stochastic approach to subsurface flow, Int. Assoc. of Hyraul. Res., Montvillargenne, France, June 3-6.
- Alt, D., and Hyndman, D.W., 1986. Roadside Geology of Montana. Mountain Press Publishing Company, Missoula, MT., pp.75-76.
- Anderson, M.P., 1984. Movement of contaminants in groundwater: Groundwater Transport - Advection and Dispersion. Groundwater Contamination (Studies in Geophysics), pp. 37-45.
- Armstrong, K.G., 1991. The Distribution and Occurence of Perchloroethylene in the Missoula Valley Aquifer. Univ. of Montana, Master's thesis, Dept. of geology, unpublished, pp 134.
- Bilings, J.B., 1992. Evaluating methods of determining the Hydraulic Conductivity distribution in a Heterogenous Unconfined Aquifer. Univ. of Montana, Master's thesis, Dept. of Geology, unpublished, pp 192.
- Clark, K.W., 1986. Interactions between the Clark Fork River and Missoula Aquifer, Missoula County, Montana. Univ. of Montana, M.S. Thesis, Dept. of Geology, unpublished, pp

- Davis, A.D., 1986. Deterministic Modeling of Dispersion in Heterogeneous Permeable Media, *Ground Water*, v. 24, no. 5, pp. 609-615.
- Dougherty, D.E., and A.C. Bagtzoglou, 1993. A caution on the regulatory use of numerical solute transport models, *GroundWater*, v. 31, no. 6, pp. 1007-1010.
- Fetter, C.W., 1993. *Contaminant Hydrogeology*. Macmillan Publishing company, New York, chapter 2.
- Goode, D.J., and L.F. Konikow, October 1990, Apparent dispersion in transient groundwater flow. *Water Resources Research*, v. 26, no. 10, pp. 2339-2351.
- Goode D.J., and L.F. Konikow, 1990. Reevaluation of large-scale dispersivities for a waste chloride plume: effects of transient flow. *ModelCARE 90: Calibration and reliability in groundwater modelling*. IAHS Publ. no. 195, pp. 417-426.
- Goode, D.J., 1992. Modelling transport in transient groundwater flow : An unacknowledge approximation, *Ground Water*, v. 30, no. 2, pp. 257-261.
- McDonald and Harbaugh, 1988. A Modular Three Dimensional Finite-Difference Groundwater Flow Model (MODFLOW), *Techniques of Water Resources Investigation of the USGS, Book 6, Modelling Techniques, Chapter A1*.
- Miller, R.D., 1991. A numerical flow model of the Missoula Aquifer : Interpretation of Aquifer properties and river

- interaction. Univ. of Montana, Master's thesis, unpublished, pp. 301.
- Molz, F.J., O. Guven, and J.G. Melville, 1983. An examination of scale-dependant dispersion coefficients, *Ground Water*, v. 21, no. 6, pp. 715-725.
- Naff, R.L., T.C.J. Yeh., and M.W. Kemblowski, 1989, Reply, *Water Resources Research.*, v. 25, no. 12, pp. 2523-2525.
- Pottinger, M.H., 1988. The source, fate and movement of herbicides in an unconfined sand and gravel aquifer in Missoula, Montana, Univ. Of Montana, Master's thesis, Dept. of Geology, unpublished, total pages 172.
- Prickette, T.A., and Lonquist, C.G., 1971. Selected digital computer techniques for groundwater evaluation, *Illinois State Water Survey Bulletin* 55, pp 62.
- Robertson, J.B., 1974. Digital modelling of radioactive waste and chemical transport in the Snake River Plain Aquifer at The National Reactor Testing Station, Idaho. USGS Open File Rep. IDO-22054.
- Sauty, J.P., 1980. An analysis of hydrodispersive transfer in aquifers, *Water Resources Research*, v. 16, n. 1, pp. 145-158.
- Sudicky, E.A., 1986. A natural gradient experiment on solute transport in a sand aquifer : Saptial variability of hydraulic conductivity and its role in the dispersion process, *Water Resources Research*, v. 22, n. 13, pp. 2069-2082.

Zheng, C., 1990. MT3D - A Modular Three-Demensional Transport Model for Simulation Of Advection, Dispersion and Chemical Reactions of Contaminants in Groundwater Systems. S.S.Papadoupulos & Associates, Inc. Rockville, Maryland 20852.

Zou, S., and A. Parr, 1993. Estimation of dispersion parameters for two-dimensional plumes, Ground Water, v. 31, no. 3, pp. 389-392.

**APPENDIX A - Input parameters and files to Flow
and Solute Transport Model # 1**

Values for the input parameters : Model # 1

Grid size = 47 rows, 52 columns

Cell width along rows = 500 feet

Cell width along columns = 500 feet

Layer thickness = 270 feet

Hydraulic Conductivity = 700 ft/d

Porosity = 0.2

Longitudinal dispersivity = 10 feet

Ratio of horizontal and vertical transverse to longitudinal
dispersivity = 0.1

Input concentration (slug injection) = 1000 mg/l

Simulation time = 3 years

Input Files : Flow Model # 1

BAS1 - Basic file

BCF1 - Block centered flow file

WEL1 - Well file (simulating Grant Creek)

RIV1 - River file (simulating Clark Fork River)

GHB1 - General head boundary file

SIP1 - Successive iteration file

OC1 - Output control file

Input Files : Solute Transport Model # 1

BTN1 - Basic transport file

ADV1 - Advection file

DIS1 - Dispersion file

SSM1 - Sink and source mixing file

SC1 - Starting concentration file

Note : All flow and solute transport files input files for
Model # 1 on Plate 1.

**APPENDIX B - Input Parameters and Files to Flow
and Solute Transport Model # 2**

Values for the input parameters : Model # 2

Grid size = 70 rows, 70 columns

Cell width along rows = 100 feet

Cell width along columns = 100 feet

Layer thickness = 270 feet

Porosity = 0.2

Longitudinal dispersivity = 10 feet

Ratio of horizontal and vertical transverse to longitudinal dispersivity = 0.1

Input concentration (slug injection) = 1000 mg/l

Simulation time = 3 years

First Scenario

Hydraulic Conductivity = 700 ft/d (Constant)

Second Scenario

Hydraulic Conductivity = varying (see input file BCF2)

Third Scenario

Hydraulic Conductivity = 700 ft/d

Constant head boundaries at column 30 and column 49, from row 1 to row 70.

Input Files : Flow Model # 2

BAS2 - Basic file (first and second scenario)
BAS3 - Basic file (third scenario)
BCF2 - Block centered flow file (first and third scenario)
BCF3 - Block centered flow file (second scenario)
GHB2 - General head boundary file
SIP1 - Successive iteration file
OC1 - Output control file

Input Files : Solute Transport Model # 2

BTN2 - Basic transport file
ADV1 - Advection file
DIS1 - Dispersion package
SSM2 - Sink and source mixing package (first and second scenario)
SSM3 - Sink and source mixing package (third scenario)
SC2 - Starting concentration file

Note : All flow and solute transport input files for Model # 2 on Plate 1.

**APPENDIX D - Input Parameters and Files to Flow
and Solute Transport Model # 3**

Values for the input parameters : Model # 3

Grid size = 70 rows, 70 columns

Cell width along rows = 100 feet

Cell width along columns = 100 feet

Layer thickness = 270 feet

Hydraulic Conductivity = 700 ft/d

Porosity = 0.2

Longitudinal dispersivity = 10 feet

Ratio of horizontal and vertical transverse to longitudinal dispersivity = 0.1

Input concentration (slug injection) = 1000 mg/l

Simulation time = 3 years

Input Files : Flow Model # 3

BAS - Basic file
BCF - Block centered flow file
SHD - Starting head file
GHB - General head boundary file
SIP - Successive iteration file
OC - Output control file

Input Files : Solute Transport Model # 1

BTN - Basic transport file
ADV - Advection file
DIS - Dispersion file
SSM - Sink and source mixing file
SC - Starting concentration file

Note : All flow and solute transport input files for
Model # 3 on Plate 1.